Doctoral Thesis

博士論文

Study on PRMT5 role in bovine leukemia virus (BLV) infection

（牛白血病ウイルス（BLV）感染における PRMT5 の生理的意義に関する研究）

Wlaa Assi

ワラ アーシー

Doctoral Thesis

博士論文

Study on PRMT5 role in bovine leukemia virus (BLV) infection

(牛白血病ウイルス(BLV)感染における PRMT5 の生理的意義に関する研究)

Wlaa Assi　ワラ アーシー

The University of Tokyo
Graduate School of Frontier Science
Department of Computational Biology and Medical Sciences

2020/06/12

Table of Contents

1 Abbreviations

SBL: Sporadic bovine leukosis

EBL: Enzootic bovine leukosis

BLV: Bovine leukemia virus

PL: Persistent lymphocytosis

HTLV-1: Human T-cell leukemia virus type 1

ATL: Adult T-cell leukemia

ORFs: Open reading frame

LTR: Long terminal repeat

MA: Matrix

CA: Capsid

NC: Nucleocapsid

PRO: Protease

Env: Envelope

SU: surface glycoprotein

TM: transmembrane glycoprotein

ITAMs: Immunoreceptor tyrosine-based activation motif

CAT1: cationic amino acid transporter 1

REFs: Rat embryo fibroblast

miRNA: microRNA

PVL: Proviral load

LPVL: low proviral load cattle

HPVL: high proviral load cattle

PBMCs: Peripheral blood mononuclear cells

TNF: Tumor necrosis factor

BoLA: Bovine leukocyte antigen

PRMTs: Protein arginine methyl transferases

PRMT5: Protein arginine methyl transferase 5

MMA: Monomethylarginine

aDMA: asymmetrical dimethylarginine

sDMA: symmetrical dimethylarginine

T: Threonine

R: Arginine

WD45/MEP50: WD repeat domain 45/methylosome protein 50

IRES: Internal ribosome entry site

H2AR3: Arginine 3 of Histone 2A

H4R3: Arginine 3 of Histone 4

H3R8: Arginine 8 of Histone 3

H4R3me2s: Symmetric di-methylation of Arginine 3 of Histone 4

H4R3me2a: Asymmetric di-methylation of Arginine 3 of Histone 4

H3K4me3: H3K4 trimethylation H4K5: Lysine 5 of Histone 4

snRNP: Small Nuclear ribonucleoproteins

HR: Homologous recombination

EGFR: Epidermal growth factor receptor

PDGFRα: Platelet-derived growth factor receptor- α

LuSIA: The luminescence syncytium induction assay

7-AAD: 7-amino-actinomycin D

HDV: hepatitis delta virus

EBV: Epstein-Barr virus

HBV: Hepatitis B virus

KSHV: Kaposi's sarcoma associated herpesvirus

HIV: Human immunodeficiency virus

HBc: hepatitis B virus core

GRE: glucocorticoid response element

EGFP: enhanced green fluorescent protein

siRNA: small interfering RNA)

LuSIA: Luminescence syncytium induction assay

qRT-PCR: Quantitative reverse transcription-polymerase chain reaction

SDS-PAGE; SDS-polyacrylamide gel electrophoresis

Mab: Monoclonal antibody

PI: Propidium Iodide

2 Abstract

Introduction

Bovine leukemia virus (BLV), an oncogenic member of the *Deltaretrovirus* genus, infects cattle worldwide and decreases profitability in the dairy industry. Some 70% of infected cattle, the natural host of BLV, remain asymptomatic, whereas the major portion of the remaining infected cattle develops persistent lymphocytosis (PL), and only 1-5% develop leukemia/lymphoma after a 10-year or longer period of a proviral latency. Because of the limited variation in the BLV genome, host factors are believed to play a crucial role in determining the BLV infection profile.

Arginine methylation is an important posttranslational modification that plays crucial roles in chromatin regulation, transcription control, RNA processing, nuclear/cytoplasmic shuttling, DNA repair, and some other biological processes. Arginine methylation is catalyzed by the protein arginine-N-methyltransferase (PRMT) family. PRMTs are divided into four types of enzymes. Type I, the most common type of PRMTs, induces asymmetric dimethylation (aDMA); Type II catalyzes the symmetric dimethylation (sDMA); Type III produces monomethyl arginine as their final product, and Type IV is found only in fungi. In the virology field, protein arginine methylation has been determined to play critical roles in the biology of several viruses including hepatitis delta virus (HDV), hepatitis B virus (HBV), human immunodeficiency virus type-1 (HIV-1), HTLV-1, Epstein-Barr virus (EBV), and Kaposi's sarcoma associated herpesvirus (KSHV).

Research Importance and Aim

Until now, studies investigating PRMTs role in BLV biology have not been conducted; therefore, we aim to investigate the role of PRMT5, which is Type II PRMTs, in some aspects of BLV infection *in vivo* and *in vitro*. First, we focused on an investigation of the

correlation between PRMT5 expression level and BLV proviral load, which is an index of virus infectivity, in peripheral blood from infected animals with various stages, such as asymptomatic and lymphoma stages. Second, we revealed the impact of PRMT5 inhibition on BLV gene expression, gp51 glycosylation and syncytium formation. To our knowledge, this is the first study that investigates the PRMT5 role in BLV infection.

Results and Discussion

1. PRMT5 is overexpressed in BLV infected cattle with a high proviral load *in vivo*

we collected blood samples from 62 cows which were asymptomatic and did not develop symptoms of lymphoma at the time of blood collection. Firstly, we performed the CoCoMo-qPCR-2 for calculation of the BLV PVL and accordingly, the cows were classified into three groups: BLV negative cattle (Uninfected group), BLV-infected cattle with low-proviral load (LPVL group) and BLV-infected cattle with high-proviral load (HPVL group). Next, we evaluated PRMT5 expression at RNA levels by qRT-PCR. The mean fold change of PRMT5 was 1.12±0.62 in the control group, 1.18±0.64 in the LPVL group, and 1.64±0.62 in the HPVL group. PRMT5 expression is significantly higher in HPVL group than that in the uninfected group ($p = 0.0014$) and in LPVL group ($p = 0.012$).

2. PRMT5 overexpression starts from the early stage of BLV infection *in vivo*

To further investigate the role of PRMT5 in BLV infection *in vivo*, we examined whether PRMT5 is overexpressed in the early stage of BLV infection. Therefore, we performed an experimental infection of five BLV-negative Japanese black calves carrying susceptible alleles *BoLA-DRB3**1601/1601 that is connected with a high proviral load BLV infection, and we collected blood samples at different time points during the first month of infection (0, 0.5, 1, 2, 3 and 4 weeks). Then we monitored BLV PVL and the PRMT5 expression at each time point. The mean of BLV PVL was 0 copies/10^5 cells before infection (0 week), 34 copies/10^5 cells after 3 days, 1158 copies/10^5 cells after 1 week, 26760 copies/10^5 cells after

2 weeks, 90150 copies/10^5 cells after 3 weeks, and 62440 copies/10^5 cells after 4 weeks. The mean fold change of PRMT5 was 1 before infection, 1.44 after 3 days, 1.48 after 1 week, 2.6 after 2 weeks, 3.7 after 3 weeks, and 2.3 after 4 weeks. The highest expression of PRMT5 occurs during the third week (FC = 3.74, $p = 0.0008$) then it slightly drops after 4 weeks (FC = 2.3, $p = 0.01$). Of interest, a strong positive correlation is found between PRMT5 upregulation fold and BLV PVL ($r = 0.79$). We concluded that PRMT5 expression is upregulated in response to BLV infection, and its upregulation fold positively correlates with BLV PVL. Moreover, PRMT5 upregulation starts from the early stage of BLV infection rather than being established after a long period of proviral latency. Taken together, our data suggest that PRMT5 overexpression is a contributing host factor for developing and keeping BLV infection.

3. PRMT5 overexpression continues to the lymphoma stage of BLV infection *in vivo*

It is well known that PRMT5 plays a role as an oncogene protein; also, PRMT5 upregulation was determined in several human cancers, including B and T cell lymphoma. We have already showed that PRMT5 is overexpressed in clinically healthy BLV-infected cattle with HPVL. Finally, we investigated whether PRMT5 expression change in BLV infected cattle reaching the lymphoma stage of the disease. We compared PRMT5 expression at the RNA level among 3 groups of cattle: 20 BLV-negative cattle, 42 BLV-infected but clinically normal cattle and 20 BLV-infected cattle with lymphoma. PRMT5 expression fold change was 1.12±0.62 in the uninfected cattle, 1.48± 0.66 in the asymptomatic group and 2.45±1.1 in the lymphoma group. This finding strongly indicates that PRMT5 upregulation continues to the lymphoma stage of BLV.

4. PRMT5 knockdown enhances BLV gene expression *in vitro*

Next, we examined the impact of PRMT5 inhibition on BLV infection *in vitro*. To investigate the effect of PRMT5 inhibition on BLV gene expression, we knockdown PRMT5

of two cell lines by siRNA: FLK-BLV, a permanently BLV infected cell line, or PK15-BLV, a stably transfected cell line with CMVΔU3-pBLV-IF2. We measured the mRNA of two viral transcripts: *gag* that is produced un-spliced mRNA, and *tax* that is produced by the alternative splicing. In addition, we measured the protein levels by Western blotting analysis for two viral proteins (Gag p24 and Env gp51). Herein, we determined that PRMT5 knockdown enhances BLV gene expression at the transcription and the protein levels in a dose dependent manner *in vitro*. Additionally, we demonstrated that PRMT5 knockdown does not impair the gp51 expression at the cell membrane. We, thus, concluded that the observed upregulation of BLV viral proteins after PRMT5 knockdown is caused by a higher expression rate rather than an impaired protein trafficking. These results provide an evidence that PRMT5 works as a negative regulator of BLV gene expression. In addition, it might reveal one mechanism of the BLV proviral latency observed *in vivo*.

5. Selective PRMT5 inhibitor alters gp51 glycosylation processing *in vitro*

To further investigate the role of PRMT5 in BLV infection, we utilized a small molecular PRMT5 inhibitor (CMP5). By using CMP5, we also confirmed that CMP5 treatment enhances BLV gene expression. Most surprisingly, we noticed that CMP5 treatment alters gp51 electrophoretic mobility over SDS-PAGE and forms gp51 with higher molecular weight than gp51 in the untreated cells. This shift was more evident in PK15-BLV cell line. This observation inspired us to investigate the possible impact of this inhibitor on BLV envelope protein glycosylation. Thus, we used two glycosidase enzymes for further investigation; PNGase F and Endo H. Our data showed that PNGase F treatment leads to the accumulation of approximately 30-KDa product. This corresponds to the calculated molecular weight of the envelope peptide core in the absence of any glycosylation of BLV gp51. Thus, after PNGase F, change in migration pattern of gp51 is disappeared, indicating that CMP5 affects the gp51 glycosylation pattern. Endo H digestion further revealed that CMP5 treatment alters gp51

glycosylation processing. This altering differs among various cell lines; in PK15-BLV cell line, CMP5 treatment enhances gp51 glycosylation processing to form a complex type of *N*-glycan that runs slower in SDS-PAGE. In the FLK-BLV cell line, limited evidence was obtained to reveal the type of irregular *N*-glycan caused by CMP5 treatment.

Next, we examined whether CMP5 treatment affects Gag or Env intracellular localization or Env expression at the cell membrane. FLK-BLV cells were grown on coverslips in the absence (CMP5 –) or presence of 20 μM of CMP5 (CMP5 +) for 48 h; Gag and Env intracellular localization were evaluated by the fluorescence confocal microscope after the permeabilization of cells with 0.5% Triton X-100 for 5 min. Gp51 expression at the cell membrane was evaluated by fluorescence confocal microscope without the permeabilization step and by flow cytometry. We observed a large accumulation of Gag after CMP5 treatment. Additionally, the intracellular Env protein accumulated near to the nucleus after the treatment. In contrast, the cell membrane expression of gp51 was not severely affected as demonstrated by the fluorescence confocal microscopy and by flow cytometry.

6. Selective PRMT5 inhibitor impedes BLV ENV-mediated syncytia formation *in vitro*

Next, we aimed to examine the impact of the PRMT5 inhibitor, CMP5, on the syncytium formation ability. FLK-BLV cells were co-cultured with CC81-GREMG, which is a reporter cell line, in the absence or the presence of different concentrations of CMP5. Interestingly, CMP5 treatment negatively affects the syncytia formation; this was detected by the eye under the fluorescence microscope and also by the automated quantification that shows that the syncytia-counts decrease in a dose-dependent manner, showing significance at the concentrations of 10 μM ($p = 0.017$) and 20 μM ($p = 0.0002$). By contrast, the total cell count during the assay remains unaffected. These facts exclude the toxic effect of CMP5 on FLK-BLV or CC81-GREMG. CMP5 treatment did impair Env expression at the cell membrane.

Thus, CMP5 treatment likely impedes BLV-induced syncytium formation via affecting the gp51 glycosylation processing as shown in our study.

7. PRMT5 inhibitor enhances apoptosis and decreases cell proliferation of KU-1 cell line

Finally, we investigated whether PRMT5 inhibition affects bovine lymphoid cells proliferation or apoptosis. We used KU-1 cell line, which is a bovine lymphoid cell line, we showed that PRMT5 inhibitor can decrease cell proliferation and enhance apoptosis. However, further studies using more lymphoid cell lines and using BLV-negative cell lines are required to fully demonstrate the potential therapeutic effects of PRMT5 inhibitors in BLV-mediated lymphoma.

In conclusion, the present study provides the first report that determined various roles for PRMT5 in BLV infection *in vivo* and *in vitro*; our data suggest that PRMT5 upregulation might be required for the development and maintenance of BLV infection by three ways: first, in the early stage of BLV infection, PRMT5 overexpression is important to the establish the infection by ensuring the correct gp51 glycosylation. Second, in the stage of after developing BLV infection, PRMT5 upregulation is involved in the silencing strategy adopted by BLV *in vivo* to avoid the host immune response, and thus PRMT5 expression correlates with BLV proviral load that indicates the number of infected cells. Third, in the final stages of BLV infection, PRMT5 expression is further increased in order to inhibit apoptosis and enhance the cell proliferation, which contribute to the development of lymphoma.

3 Introduction

3.1 BLV introduction

3.1.1 BLV general introduction

Bovine leukosis was first described by Leisering *et al* in 1871 as the presence of slightly yellow nodules in the enlarged spleen of cattle. Bovine leukosis is classified into two types, sporadic bovine leukosis (SBL) which is T-cell leukosis and enzootic bovine leukosis (EBL), which is B-cell leukosis [1,2]. EBL prevalence in cattle is higher than that of SBL [2,3]. Bovine leukemia virus (BLV), which belongs to the *Retroviridae* family and Deltaretrovirus genus, is the etiologic agent of EBL. However, the causes of SBL remains unknown [1,2]. BLV infects cattle worldwide (**Figure 1**) and decreases profitability in the dairy industry [4]. BLV naturally infects cattle and water buffaloes. Moreover, it experimentally infects many cell lines and several animals such as rabbit, rats, chickens, pigs, goats, and sheep [2]. After BLV infection, some 70% of infected cattle, the natural host of BLV, remain asymptomatic, whereas the major portion of the remaining infected cattle develops persistent lymphocytosis (PL), and only 1-5% develop leukemia/lymphoma after a 10-year or longer period of a proviral latency [1] (**Figure 2**) . Even though, BLV can experimentally infects several animal species, only cattle and sheep may develop leukemia after BLV infection. Additionally, B-cell tumors in sheep is developed at a higher frequency and with a shorter latency period than that observed in cattle [5–8]. Of note, the transformed B-cells in cattle are $CD5^+$ IgM^+ B-cells [9], whereas in sheep they are $CD5^-$ IgM^+ B-cells [10]. BLV is closely related to human T-cell leukemia virus type 1 (HTLV-1), which is the causative agent of adult T-cell leukemia (ATL) [1,2].

BLV transmission occurs through horizontal, which is the major route, and vertical transmissions. BLV is transmitted horizontally through direct contact in insect-free condition

[11], milk [12], and insect bites [13]. Additionally, the artificial transmission of BLV occurs via iatrogenic procedures including: dehorning, ear tattooing, and reuse of needles [14]. Because the virion particles are instable, cell-free infection is inefficient and BLV transmits mainly via cell-to-cell infection. Thus, cell contact is required for the efficient transmission of BLV [2].

BLV can infect several cell types in cattle including: $CD4^+$ T-cells, $CD8^+$ T-cells, γ/δ T-cells, monocytes, and granulocytes. Nevertheless, BLV induces malignancy mainly in $CD5^+$ IgM^+ B-cell sub-population [2].

3.1.2 The BLV genome, RNA transcripts, and the viral proteins

The full genome of BLV is comprised of 8714 nucleotides [15]. BLV genome (Figure 3) is flanked between two identical long terminal repeat sequences (LTRs) and contains the open reading frames (orfs) corresponding to the structural genes *gag*, *pro*, *pol* and *env*, which is required for the synthesis of the viral particles. In addition to the structural genes, the BLV genome contains a pX region located between the *env* gene and the 3'LTR. The pX region contains the regulatory genes *tax*, *rex*, *R3*, and *G4* [1,2]. The BLV genomic RNA serves as a template for the expression of the gag-pro-pol precursors (pr145, pr66 and pr44) that are processed in structure and enzymatic proteins: matrix (MA) p15, capsid (CA) p24, nucleocapsid (NC) p12, protease (PRO) p14 and, p80 (RT/IN) that have reverse transcriptase, RNAse H and integrase activities [1]. The mRNA-*env* of BLV encodes a Pr72 envelope (Env) precursor that is glycosylated in the rough endoplasmic reticulum and Golgi apparatus [16,17]. This precursor is cleaved by cellular proteases into two mature proteins–the surface subunit gp51 and transmembrane subunit gp30–which are associated by disulfide bonds [17,18]. The surface subunit gp51 is highly immunogenic, a strong neutralizing antibody against gp51 emerge after BLV infection. The monoclonal antibodies targeting the epitope H

completely inhibited the cell fusion ability of BLV. Additionally, antibodies targeting F and G epitopes were efficient in reducing the syncytia formation ability. The simultaneous loss of these three epitopes (H, F, and G) was not reported in all known BLV strains, thus these epitopes are believed to play critical role in BLV life cycle [19,20]. In addition to the three conformational epitopes (H, F, and G) [21], the gp51 also contains four linear epitopes (A, B, D, and E) in its C-terminus [20]. Moreover, the gp51 has B cell epitope that is important for the use of antibodies as therapeutic agents, the epitope-driven vaccine design, and immunological assays [22].

Besides the humoral immune response, the gp51 also contains $CD4^+$ and $CD8^+$ cell epitopes, hence stimulates a T-cell response [23,24]. The BLV-gp51 is highly glycosylated and it has eight potential *N*-glycan sites. The role of these glycosylation sites in BLV pathogenicity was determined using reverse genetics. It has been shown that the simultaneous mutation of the eight N-glycosylation sites abrogates the viral infectivity *in vivo*. On the other hand, all single mutations at *N*-glycan sites, except for N230, are almost silent. Interestingly, this N230 mutation stabilizes the gp51 and enhances the cell-to-cell infection *in vitro*. Moreover, the BLV provrirus that carries the N230 mutation replicates faster than the wild-type and it is more pathogenetic than the wild-type [25]

In contrast to the surface glycoprotein (SU) subunit gp51, the transmembrane glycoprotein (TM) subunit gp30 is poorly immunogenic. gp30 contains three distinct domains: the fusion peptide that is the extracellular domain and interacts with gp51 [26], a membrane spanning domain that anchors the gp51-gp30 complex in the cell membrane or viral membrane [18], and the cytoplasmic tail that contains three YXXL sequences, which were originally identified as immunoreceptor tyrosine-based activation motif (ITAMs) [22]. The biological roles of YXXL sequences in BLV life cycle have been thoroughly identified [28,29].

The gp51 binds to the cationic amino acid transporter 1 (CAT1)/SLC7A1, which is the newly identified BLV receptor and it is responsible for BLV broad host range [30]. After gp51 binding to the cellular receptor, the disulfide bond linking SU and TM is broken and consequently the conformational change of TM lead to exposing the fusion peptide of TM to initiate the fusion process. The fusion peptide in N-terminus of TM destabilizes the cell membrane and disrupts the lipid bilayer, which allows the release of the viral NC into the host cytoplasm. This process requires forming a six-helix coiled coil bundle that triggers the fusion of viral and cell membrane by bringing them in a close distance [16,31].

Tax/Rex mRNAs are produced by a double splicing event. This double-spliced RNA encodes both the p34 Tax protein and Rex proteins using two different initiation codons. Two additional viral transcripts, R3 and G4, are produced by further alternative splicing events. Whereas the structural genes encode for proteins required for production of virus particles, the pX region encodes accessory proteins that are important for inducing BLV-mediated pathogenesis. Tax protein is believed to play crucial role in BLV-induced leukemogenesis [32,33]. The Rex protein functions in nuclear export of viral RNA and it induces cytoplasmic accumulation and translation of viral mRNA [34]. The R3 and G4 proteins play a role in the maintenance of high viral load and deletion of the R3 and G4 sequences from an infectious and tumorigenic BLV provirus impaired the *in vivo* propagation of the viruses [35,36]. The G4 protein exhibits oncogenic potential because it can immortalize primary rat embryo fibroblast (REFs). Thus, it might be involved in the leukemogenesis process [37].

Besides the transcripts that express the viral proteins, BLV RNA polymerase III (pol III)-encoded viral microRNAs (miRNA) are strongly expressed in preleukemic and malignant cells, in which structural and regulatory gene expression is repressed, indicating a potential role in tumor onset and progression [38,39]. Indeed, it has been demonstrated that BLV-miRNAs regulate the expression of genes involved in cell signaling, tumor and immunity.

Furthermore, BLV miRNAs are critical to induce B-cell malignancy and to induce efficient viral replication in the natural host [40].

3.1.3 The BLV virion

The BLV virion (**Figure 4**) has a diameter ranging between 60 and 125 nm. It is formed by a central electron dense nucleoid surrounded by viral envelope protein. The infectious virion contains 60–70 S ribonucleic acids that result from the binding of two 38 S poly-A containing RNA molecules [1].

The BLV virion particle consists of two copies of single stranded genomic RNA. The genomic RNA interacts with MA p15 and NC p12 proteins and dimerizes by a region surrounding the primer binding site [35]. Two regions are required for an efficient encapsidation of the viral RNA: a primary signal that is located in the untranslated region between the primer binding site and near *gag* start codon and a secondary signal, which is a 132-nucleotide-base region within the 5' end of the *gag* gene [42]. Moreover, viral RNA packaging requires the involvement of both the MA and NC domains of Pr145gag-pol [43]. The CA (p24) protein forms the capsid. The virion also has two enzymatic proteins which are RT that is required for the reverse transcription and the IN that is required for the integration. The matrix protein MA (p15) interconnects the capsid and the outer viral envelope. The viral envelope is formed by a lipid bilayer originated from the host cell membrane in addition to the inserted viral Env that has two subunits (gp51 SU and gp30 TM). The viral RNA can either be directly translated to yield the $Pr145^{gag\text{-}pol}$ precursor or incorporated into new viral particles (**Figure 5**).

3.1.4 BLV proviral load (PVL)

BLV PVL correlates strongly not only with the BLV infection capacity as assessed by syncytium formation [44,45], but also with BLV disease progression [44,46,47]. For example, BLV-infected cattle at the PL stage are known to carry a significantly increased number of PVL compared to the number of the PVL in aleukemic cattle. A further increase was observed at the lymphoma stage [44,46]. Additionally, BLV PVL is a useful index for estimating transmission risk [48]. A previous report predicted that as determined by the BLV-CoCoMoqPCR-2 method which involves quantitative measurement of PVL [44,49], cows with a PVL of greater than 14,000 copies/10^5 cells in their blood samples secreting BLV provirus into nasal were classified as having a high-PVL (HPVL) [50]. Furthermore, the BLV provirus was detected in milk samples from dams at a PVL of approximately >10,000 copies/10^5 cells in the blood [12]. These cows may have a high risk of BLV transmission through direct contact with healthy cows. In contrast, cattle with low-PVL (LPVL) are known to prevent natural BLV infection [51].

3.1.5 BLV proviral latency and antisense BLV transcription

BLV maintains in a silent state *in vivo*, and the expression of the viral proteins is blocked at the transcription level [52,53]. It has been shown that the BLV gene transcription in fresh tumor cells or fresh peripheral blood mononuclear cells (PBMCs) from infected cattle is undetectable using the conventional method such as hybridization [52,54,55]. This proviral latency enables the virus to escape from the host's immune defense, and later some population reach the terminal stage of the disease [1,2]. Even though BLV expression is almost undetectable in BLV-infected cattle *in vivo*, a strong cytotoxic and humoral immune responses are induced during the infection. Furthermore, BLV expression can be reactivated after *ex vivo* culture just after incubation of whole blood at 37°C without addition of any

factor except anticoagulants [55]. BLV latency, thus, became a standing dogma. The presence of a strong anti-viral immune response in infected animals suggests that viral proteins must be expressed in some infected cells. Therefore, it has been suggested that viral expression occurs in a subpopulation of infected cells, these cells, however, are efficiently removed by the immune system. On the other hand, the viral transcription in a subpopulation of infected cells are silenced, thereby, avoid the cytotoxic and humoral response [1].

It has been recently determined that BLV expresses antisense transcripts from the 3'LTR in all asymptomatic and leukemic infected cattle. The detailed role of these antisense RNA transcripts in the biology of BLV has not been fully understood. The antisense transcripts are retained in the nucleus, suggesting that they may have a long noncoding RNA-like role. Additionally, these transcripts may share a transcriptional interference role with the microRNA in the regulation of BLV infection [56]. It has been recently proved that BLV provirus is preferentially integrated near cancer driver genes and perturb their expression by either provirus-dependent transcription termination or as a result of viral antisense RNA-dependent cis-perturbation [57].

3.1.6 BLV replication

There are two main ways for BLV replication: infectious cycle or mitotic cycle. The infectious cycle occurs in the early stage of the infection before the onset of an efficient immune response, and it includes infection of the target cells by the virion, reverse transcription of the viral RNA to DNA, and integration of the viral DNA into the host genome as a provirus (**Figure 5**). Thus, at the early stage of infection, multiple clones are generated. Once the cellular and humoral specific immune responses are elicited (4-8 weeks post-infection), a strong reduction of these initial clones occurs, and the infection then

spreads through clonal expansion of infected host cells (mitotic cycle), without reverse transcription [58–60].

3.1.7 Role of host factors in BLV pathogenesis

BLV-mediated pathogenicity depends on a delicate balance between viral gene expression and certain host-related genetic and epigenetic events [2]. The mutation rate of BLV is relatively low [61] and spontaneous variations in the BLV genome have a limited impact on the biological properties of the virus [62]. Thus, host factors are thought to play crucial roles in determining the BLV infection profile. The protein encoded by p53 tumor suppressor gene, Bovine leukocyte antigen (*BoLA*) gene, and the tumor necrosis factor (*TNF*)-α gene are a notable examples of host factors that affect BLV infection.

The protein encoded by p53 tumor suppressor is critical for inducing the signal from the damaged DNA to the genes that regulate cell cycle and apoptosis. It had been reported that about five of ten BLV-induced bovine tumors harbored p53 mutations [63–65]. On the other hand, only one of seven samples in B-cells from cows with PL showed an alteration of the p53 gene [63]. Moreover, four of eight bovine-cell lymphoma lines harbor missense mutations in p53 [66]. Notably, p53 mutations were not found in BLV-induced sheep tumors, indicating that p53 mutations frequently occur in cattle at the final stage of lymphoma, and it might reflect different molecular mechanisms involved in BLV-induced pathogenesis in sheep and in cattle [63].

BoLA plays an important role in BLV infection profile and tumor development [67,68]. *BoLA-DRB3* is the most functionally important and the most polymorphic *BoLA* class II locus in cattle. Several studies have identified *BoLA-DRB3* alleles and single-nucleotide polymorphisms in the *BoLA* region that are associated with BLV PVL and disease progression [46,69–74]. For instance, it has been shown that the amino acids Glu-Arg (ER) at

the position 70-71 of *BoLA-DRβ* chain is related to the resistance to develop persistent lymphocytosis in the BLV-infected cattle [75].

The polymorphism in the promoter of the *TNF-α* gene is another host factor that affects the BLV-mediated lymphoma development. For example, the *TNF-α*-824G allele is related to weak transcription activity of the promoter region of the bovine *TNF-α* gene. It has been reported that the frequency of this allele is higher in the experimentally infected sheep that developed lymphoma than that in the asymptomatic animals. Furthermore, infected cattle carrying homozygous *TNF-α*-824G/G allele have increased proviral load compared to the cattle carrying homozygous *TNF-α*-824A/A or *TNF-α*-824A/G alleles. These facts indicate that the polymorphism in the promoter region of the *TNF-α* gene contributes to the progression of lymphoma in BLV infection [76].

3.2 Protein Arginine Methyltransferases (PRMTs)

3.2.1 PRMTs general introduction:

Arginine is a α-amino acid that is used in the biosynthesis of the proteins. The arginine side chain has a guanidinium moiety that makes it positively charged at physiological PH. The guanidinium moiety favors π- stacking interactions with aromatic rings and can form five hydrogen bonds. Arginine has the highest pKa value among all amino acids (about 13.8). Arginine residues are post-translationally modified to include methyl groups, resulting in monomethylarginine (MMA), asymmetrical dimethylarginine (aDMA) or symmetrical dimethylarginine (sDMA). Even though the methylation of arginine maintains its positive charge, it reduces its hydrogen bonding capacity by removing a hydrogen atom for each added methyl group. Moreover, the methyl group adds hydrophobicity to the side chain, thereby favoring interactions with aromatic cages [77].

Arginine methylation is an important post-translational modification found on both nuclear and cytoplasmic proteins. The methylation of arginine residues is catalyzed by a family of enzymes called protein arginine *N*-methyltransferase (PRMTs) [78]. Arginine methylation is involved in the regulation of fundamental cellular processes, including transcription regulation, RNA processing, signal transduction, and DNA damage response. PRMTs methylate glycine and arginine-rich motifs (GAR motifs) within their targets. Arginine methylation is classified into three types (**Figure 6**): MMA, sDMA and aDMA, each of which is catalyzed by a specific type of PRMTs family [79]. PRMT5 is the major type II mammalian enzyme activity, which produces symmetric demethylation arginine

3.2.2 PRMT5 regulation

PRMT5 was originally identified as Janus kinase binding protein 1 [80] and it is found to be phosphorylated by JAK2-V617F, which is JAK 2 mutant kinase found in most cases of the myeloproliferative neoplasm. PRMT5 phosphorylation by JAK2-V617F downregulates its methyltransferase activity and affects chromatin modification and gene expression mediated by PRMT5 [81]. It is also shown that PRMT5 is regulated by phosphorylation at threonine 80 (T80) that is mediated by RhoA-activated kinase in hepatocellular carcinoma cells, this phosphorylation increases PRMT5 methyltransferase activity. The myosin phosphatase (MP) holoenzyme inhibits PRMT5 T80 phosphorylation [82]. PRMT5 is also phosphorylated by liver kinase B1 (LKB) on T132, T139 and T144, and this phosphorylation is required for PRMT5 methyltransferase activity in breast cancer [83]. Additionally, the phosphorylation of the PRMT5 carboxy-terminal residue T634 by AKT/SGK kinases regulates its interaction with either PDZ (one of the most abundant protein domains found in multicellular eukaryotes) or 14-3-3 proteins (readers of phospho-serine/threonine motifs) in which, the unphosphorylated C-terminal tail binds PDZ domains, and the phosphorylated tail binds 14-

3-3- proteins. The PDZ–PRMT5 interaction is critical for facilitating the plasma membrane association of PRMT5 and consequently conducting cytoplasmic functions such as the methylation of the cytoplasmic tail of receptors. Therefore, the transgenic mice expressing C-tail truncated PRMT5 are not compatible with life because the last few amino acids of C-terminal tail of PRMT5 are important during the embryogenesis [84]. Finally, PRMT5 forms a complex with WD45/MEP50 (WD repeat domain 45/methylosome protein 50) and with either pICln (chloride channel nucleotide sensitive 1A) or serine/ threonine-protein kinase RIO1 (RIOK1), which regulate the methyltransferase activity and substrate specificity of PRMT5 [85]. Phosphorylation of MEP50 at T5 by cyclin-dependent kinase 4–cyclin D1 (Cyclin D1/CDK4) enhances PRMT5 activity and promotes neoplastic growth [86]. Besides phosphorylation, PRMT5 can be regulated by ubiquitylation. In hepatocellular carcinoma, PRMT5 undergoes polyubiquitylation both *in vitro* and *in vivo*, the polyubiquitylation of PRMT5 by E3 ubiquitin-protein ligase CHIP leads to its proteasomal degradation. Therefore, downregulation of CHIP and overexpression of PRMT5 have been observed in several human cancer [87]. This degradation process of PRMT5 is regulated by a long intergenic non-coding RNA (LINC01138), which interacts with PRMT5 and enhances its protein stability by blocking ubiquitin/proteasome-dependent degradation [88]. PRMT5 is also regulated by miRNAs; in glioma cells, miR-4518 targets the PRMT5 mRNA. The long non-coding RNA SNHG16 acts as an oncogenic lncRNA that promoted glioma tumorigenesis via acting as a competing endogenous RNA that regulates the expression of PRMT5 through directly sponging miR-4518. Decreased expression of SNHG16 increases the availability of miR-4518 and thus decreases PRMT5 expression, leading to cell growth arrest and apoptosis [89].

3.2.3 Cellular roles of PRMT5

3.2.3.1 Transcription

PRMT5 symmetrically dimethylates H2AR3, H4R3 and H3R8 to mediate transcriptional repression [80,90]. There is a cross-talk between histone arginine methylation and lysine acetylation. For example, PRMT5-mediated H4R3me2s is associated with reduced histone tail acetylation (H4K5) and thus with transcriptional repression [91]. By contrast, the PRMT1-mediated H4R3me2a is associated with hyperacetylation and transcription activation [92]. Additionally, PRMT5-mediated H3R2me2s favors WDR5 recruitment to the histone H3 and subsequently produces H3K4 trimethylation (H3K4me3), which is connected with active transcription [93]. Of note, this is mechanistically important in breast cancer stem cells, because H3R2me2s-mediated PRMT5 on *FOXP1* promoter facilitates WD repeat domain 5 (WDR5) recruitment, thereby H3K4me3 production, and enhances gene expression [94]. In contrast to PRMT5, PRMT6-mediated H3R2me2a inhibits transcription by preventing WDR5 binding to H3 [95,96].

3.2.3.2 Splicing

PRMT5 is an essential regulator of splicing in mammals, PRMT5 methylate three Sm proteins, which bind to different small nuclear RNAs [97,98]. These methylated Sm proteins are recognized by the tudor domain of survival motor neuron (SMN), the spinal muscular atrophy gene product; which enhances the small nuclear ribonucleoproteins (snRNPs) maturation [97–100]. PRMT5 depletion results in reduced methylation of Sm proteins, irregular constitutive splicing, and the alternative splicing of specific mRNAs with weak 5′ donor sites [101]. Moreover, PRMT5 depletion in neural stem cells or progenitor cells causes mis-splicing of hundreds of genes that play roles in regulating cell proliferation and signaling [101]. One of the notable examples of the genes that is affected by PRMT5 depletion is

MDM4, which is a repressor of p53 pathway. *MDM4* can express a functional full length *MDM4*, or a short isoform that is unstable and targeted for degradation by nonsense-mediated mRNA decay pathway [101,102]. PRMT5 inhibition leads to a reduction in symmetrical dimethylation of Sm proteins and thereby enhancing producing the expression of the short *MDM4* isoform and consequently, relief of repression of the p53 pathway [101]. This mechanism has been found in several human malignancies, including melanoma and hematological malignancies [103–105]. Besides the mis-splicing of *MDM4* resulted from PRMT5 depletion, the lysine acetyltransferase TIP60 (KAT5) is alternatively spliced in hematopoietic progenitor cells upon PRMT5 inhibition, which impairs the homologous recombination (HR) repair [106].Moreover, PRMT5 inhibition affects the splicing of key components of cytokine signaling pathway in immune cells leading to reduction in number and function of natural killer cells and other T cells [107]. In addition to the role of PRMT5 in regulation the splicing fidelity by the methylation of Sm proteins in the cytoplasm, PRMT5 methylate zinc finger protein 326, thereby ensuring the correct exclusion of AT-rich exons. PRMT5 inhibition leads to defects in alternative splicing, including the inclusion of AT-rich exons, which in turn leads to aberrant destabilization of mRNA of some breast cancer oncogenes such as *FOXM1* and *AP4* [108].

3.2.3.3 Translation

PRMT5 methylate several RNA binding proteins (RBPs) that are critical to achieve mRNA translation. PRMT5 facilitates the translation of a subset of internal ribosome entry site (IRES)-containing genes. Therefore, PRMT5 depletion lowers the protein expression of (IRES)-containing mRNA such as MEP50, CCND1, MYC, HIF1a, MTIF and CDKN1B [109]. Additionally, the heterogeneous nuclear ribonucleoprotein A1 (hnRNP A1), an IRES transacting factor, is methylated by PRMT5 at R218 and R225, and this methylation is

critical to facilitate its interaction with IRES-containing RNAs in order to promote protein synthesis [109]. Moreover, PRMT5 interacts with and methylate the ribosomal protein S10 (RBS10) at R158 and R160. Thus, PRMT5 regulates general mRNA translation because PRMT5-mediated RPS10 methylation is required for efficient assembly of S10 into ribosomes [110].

3.2.3.4 The DNA damage response

PRMT5 has been addressed as an oncoprotein. PRMT5 is overexpressed in several cancer and PRMT5 inhibition affects cancer cell growth by different mechanisms including: cell cycle arrest, spontaneous DNA damage, defects in homologous recombination HR and aberrant p53 activation (reviewed in [111]). PRMT5 regulates HR via the methylation of R205 of the AAA+ ATPase RUVBL1 which is a subunit of the TIP60 complex [112]. At double-strand break (DSB) sites, PRMT5-directed methylation of RUVBL1 is required for the acetylation of H4K16 by TIP60, this blocks the binding of the tandem Tudor domains of the DNA-resection inhibitor 53BP1 at neighboring H4K20me2, thereby favoring DSB repair by HR over non-homologous end joining [112]. Notably, PRMT5-deficient hematopoietic progenitor cells have reduced TIP60 acetyltransferase activity and thus defective homologous recombination (HR). These cells display aberrant splicing of the TIP60/KAT5, which affects its lysine acetyltransferase activity and leads to impaired HR [106]. Additionally, PRMT5 methylate and regulates the function of several proteins that play roles in DNA damage response such as, flap endonuclease 1 (FEN1) [113], cell cycle check-point control protein RAD9 [114], and tyrosyl- DNA phosphodiesterase (TDP) [115].

3.2.3.5 Signaling pathways

PRMT5 regulates NF- κB through methylation the p65 subunit of NF- κB on R30 and thus facilitating NF-κB-induced gene expression [116]. Moreover, PRMT5 regulates the transforming growth factor- β (TGFβ–SMAD) signaling, which represses the expression of some transcription factors that are critical for melanogenesis. PRMT5 complex containing SHARPIN methylate the transcriptional co-repressor SKI, SKI is known to repress TGFβ–SMAD signaling. This counteracts the inhibition of the related transcription factors, thereby, promotes their expression and induces melanoma growth [117,118].

PRMT5 regulates ERK activity in which cells with high PRMT5 levels have lower ERK activity. This is catalyzed via methylation the R1175 of epidermal growth factor receptor (EGFR) by PRMT5. This methylation positively modulates EGF-induced EGFR trans-autophosphorylation at Tyr 1173, which governs ERK activation. Protein-tyrosine phosphatase SHP1 associates with phosphorylated Y1173 and dephosphorylates components of the RAS–RAF–ERK signaling pathway to inhibit their function. Thus, PRMT5 inhibition enhances EGF-stimulated ERK activation by reducing SHP1 recruitment to EGFR. Additionally, PRMT5 methylate RAF proteins, which negatively affects their stability. Overall, PRMT5 inhibits the EGFR–ERK pathway by methylation both EGFR and its effectors [119].

PRMT5 methylate the platelet-derived growth factor receptor- α (PDGFRα) at R554. In mice, deletion of PRMT5 in oligodendrocyte precursor cells decreases the availability of PDGFRα at the plasma membrane due to increased degradation by the Cbl E3 ligase, thereby impairs axon myelination in the central nervous system [120].

3.2.4 The role of PRMT5 in viruses' life cycle

PRMT5 was recently shown to play a critical role in EBV-driven B-cell transformation [121] and HTLV-1-mediated T-cell transformation [122]. PRMT5 regulates various steps in

virus lifecycles. For example, PRMT5 restricts hepatitis B virus replication via two mechanisms: epigenetic suppression of covalently closed circular DNA and interference with pregenomic RNA encapsidation [123]. Further studies showed that PRMT5 regulates nuclear import of hepatitis B virus core (HBc) in which PRMT5 overexpression increases the nuclear accumulation of HBc, and in which PRMT5 inhibition reduces HBc levels in the nuclei [124]. Moreover, the early lytic protein of Kaposi's sarcoma associated herpesvirus, ORF59, associates with PRMT5 and disrupts its binding with the chromatin which in turn disrupts its repressive effect to move to the lytic reactivation phase [125]. It has also recently been demonstrated that PRMT5 supports HIV-1 replication by maintaining Vpr protein stability [126]. The roles of PRMT5 in viruses' life cycle are summarized in (**Table 1**)

3.3 Research aim

Even though the role of PRMT5 has been widely studied in several viruses' life cycle, it remains unclear whether PRMT5 acts as a host cell factor that is important in BLV gene expression and infection.

The aim of this study is to investigate the role of PRMT5 in various aspects of BLV infection *in vivo* and *in vitro*, and investigate the therapeutic effect of PRMT5 inhibitors as a novel anti-retroviral therapy *in vitro*.

First, we focused on examining PRMT5 dysregulation in several stages of BLV infection, and examining the correlation between the PRMT5 expression level and BLV proviral load, which is an index of virus infectivity, in peripheral blood from infected animals with various stages, such as asymptomatic and lymphoma stages. Second, we revealed the impact of PRMT5 inhibition on BLV gene expression, gp51 glycosylation, and syncytium formation. This is the first study to investigate the role of PRMT5 in BLV infection.

4 Materials and Methods

4.1 Cell culture and transfection

FLK-BLV cells, which are permanently infected with BLV (kindly provided by Prof. Onuma, M.), were cultured in Dulbecco's modified Eagle's Medium (Thermo Fisher Scientific, Waltham, MA, USA) containing 10% heat-inactivated fetal bovine serum (Sigma-Aldrich, St. Louis, MO, USA). PK15-BLV cells, which were produced by stably transfecting of the pig kidney-15 (PK15) cells (National Institutes of Biomedical Innovation, Health and Nutrition: JCRB9040) with CMVΔU3-pBLV-IF2, were cultured in Minimum Essential Medium Eagle (Thermo Fisher Scientific) containing 10% fetal bovine serum and 1% non-essential amino acids (Gibco, Grand Island, NY, USA). CMVΔU3-pBLV-IF2 is the modified version of the BLV-infectious molecular clone pBLV-IF2, which was used previously [28,30]. CMVΔU3-pBLV-IF2 was modified by replacing the U3 region that contains the BLV promoter with the strong CMV promoter to enhance BLV expression. FLK-BLV and PK15-BLV were selected because they stably express BLV-viral proteins and produce BLV-virus particles, enabling analysis of several aspects of the virus life cycle related to the expression of viral proteins.

For transfection of small interfering RNA (siRNA), we used Lipofectamine RNAiMax Reagent (Thermo Fisher Scientific) according to the manufacturers' instructions and RNA was extracted from these cells using TRIzol reagent (Thermo Fisher Scientific) according to the manufacturer's protocol.

4.2 Animal samples and isolation of genomic DNA and RNA

Blood samples were collected from 62 Holstein cattle including BLV-negative cattle and BLV-infected cattle, which were maintained in Japan. These cows were classified into three groups according to their PVL as follows: (i) BLV-negative cattle (PVL = 0; N = 20), (ii) BLV-infected cattle with LPVL (PVL ≤10,000 copies/10^5 cells; N = 15), and (iii) BLV-infected cattle with HPVL (PVL >10,000 copies/10^5 cells; N = 27). Blood samples were also collected from BLV-infected Holstein cows with lymphoma (N = 20). Lymphoma was diagnosed by both gross and histological observation and by detecting atypical mononuclear cells in the slaughterhouse. The age of animals and their individual proviral load were shown in **Table 2**. All animal experiments were conducted in accordance with the guidelines for Laboratory Animal Welfare and Animal Experiment Control established by the RIKEN Animal Experiments Committee (H29–2-104). For experimental infection, five BLV-negative one-year-old Japanese black calves carrying susceptible alleles *BoLA-DRB3*1601/*1601* were experimentally challenged intravenously with blood containing a PVL of 4×10^7 copies/10^5 cells. This study was approved by the Animal Ethical Committee and the Animal Care and Use Committee of the Kyoto Biken Institute.

Blood samples were collected and diluted in a 1:1 ratio with Ambion® nuclease-free water before adding TRIzol LS in a 3:1 ratio of TRIzol LS to the diluted whole blood. The mixtures of whole blood with TRIzol LS were transported to the lab and stored at –80°C. An equal volume of the mixture was used to extract RNA from the samples using TRIzol LS protocol (Thermo Fisher Scientific) according to the manufacturer's instructions.

4.3 Measurement of the BLV PVL

The BLV PVL was measured by BLV-CoCoMo-qPCR-2 (RIKEN Genesis, Kanagawa, Japan) using genomic DNA as described previously [49]. Briefly, the BLV LTR region was amplified in a reaction mixture containing THUNDERBIRD Probe qPCR Mix (Toyobo, Tokyo, Japan) and the degenerate primer pair: CoCoMo FRW primer and CoCoMo REV primer. FAM-LTR was used as a probe. *BoLA-DRA* (internal control) was amplified using the primer pair DRA-F and DRA-R. FAM-DRA was used as a probe. The PVL was calculated using the following equation: (number of BLV-LTR copies/number of *BoLA-DRA* copies) × 10^5 cells.

4.4 Quantitative reverse transcription-polymerase chain reaction (qRT-PCR)

RNA was reverse-transcribed for cDNA synthesis using a High Capacity RNA-to-cDNA kit (Thermo Fisher Scientific) according to the manufacturer's instructions. Primer design for PRMT5, GAPDH, *gag*, and *tax* was performed using the primer-designing tool provided by the National Center for Biotechnology Information. The primer list is shown in **Table 3**. RT-PCR was performed with the KAPA SYBR® FAST qPCR Kit (KAPA BIOSYSTEMS, Wilmington, MA, USA) using an Applied Biosystems 7500 Fast Real-Time PCR system (Foster City, CA, USA). The following thermal cycling program were used: 95°C for 3 min, followed by 40 cycles of 95°C for 10 s and 60°C for 30 s. Samples were evaluated in duplicate, and data analysis was performed using the comparative CT method (ΔΔCT) with normalization to GAPDH mRNA expression.

4.5 siRNA transfection

siRNA designed to target PRMT5 (si-PRMT5) of FLK-BLV or PK15-BLV was constructed by Silencer Select siRNAs (Ambion, Austin, TX, USA). To knockdown PRMT5 in FLK-BLV cells, Silencer® select Product # s20376 was used. For PK15-BLV knockdown, Silencer® select Product # s20377 was used. siRNA negative control (si-NC) was constructed by Ambion (catalog# 4390843). On the transfection day, 3×10^5 cells of FLK-BLV or PK15-BLV were seeded into a 6-well plate and transfected with si-PRMT5 or si-NC using Lipofectamine RNAiMAX reagent (Thermo Fisher Scientific) according to the manufacturer's instructions. After 48 or 72 h of incubation, cell lysates were prepared, and knockdown efficiency was evaluated by RT-PCR or Western blotting analysis.

4.6 PRMT5 inhibitor treatment

CMP5, a selective PRMT5 inhibitor [121], was purchased from Merck KGaA (Darmstadt, Germany). Cells were grown for 24 h at 37°C, after which the medium was collected and replaced with fresh medium with or without 5, 10, or 20 μ M of CMP5, and the cells were grown for further 24 h. After a total of 48 h, cell lysates were prepared to determine the intracellular expression by Western blotting analysis.

4.7 Western blotting analysis

Cells were lysed for 30 min on ice in 20 mM Tris-HCl (pH 7.4), 300 mM NaCl, 2 mM EDTA, and 2% NP40 supplemented with a protease inhibitor cocktail (Roche Diagnostics, Mannheim, Germany). Lysates were mixed with SDS buffer and boiled for 5 min. Protein concentrations were determined with Pierce™ BCA Protein Assay Kit (Thermo Fisher Scientific). Equal amounts of protein were electrophoresed via SDS-polyacrylamide gel

electrophoresis (PAGE). The proteins were then transferred onto a polyvinylidene difluoride membrane (Millipore, Billerica, MA, USA) using a Trans-Blot Turbo apparatus (Bio-Rad, Hercules, CA, USA) and incubated with anti-BLV gp51 monoclonal antibody (Mab) (BLV 2) (1:200; VMRD, Pullman, WA, USA), anti-BLV Gag Mab (BLV 3)(1:200; VMRD), polyclonal anti-PRMT5 (1:1000; Abcam, Cambridge, UK), or anti-α tubulin clone B-5-1-2 Mab (1:2000; Sigma). After washing, the membranes were incubated with horseradish peroxidase-conjugated AffiniPure goat anti-Mouse IgG (1:2000; Jackson ImmunoResearch, West Grove, PA, USA) or horseradish peroxidase-conjugated goat anti-rabbit IgG (1:1000; Amersham Biosciences, Amersham, UK). Signals were visualized after treating the membrane with SuperSignal™ West Pico PLUS Chemiluminescent Substrate (Thermo Fisher Scientific). Images were acquired using MultiImage TM light Cabinet (Alpha Innotech Corporation, San Leandro, CA, USA). Band intensity was quantitated using the analysis tool provided with AlphaEaseFC^{TM} software (Alpha Innotech Corporation).

4.8 Deglycosylation by PNGase F or Endo H

FLK-BLV or PK15-BLV were cultured in the absence or presence of 20 μM CMP5 for 48 h. Thereafter, the cell lysates were treated in the absence or presence of PNGase F (Promega) for 3 h or Endo H (Promega) overnight according to the manufacturer's protocol (catalog# V483A and catalog #V4871), respectively.

4.9 Cell viability assay

A Premix WST-1 Cell Proliferation Assay Kit (Takara, Shiga, Japan) was used to assess the effect of CMP5 on cell viability. For each cell line, 3×10^4 cells were seeded into a 96-

well plate at a final volume of 100 μL in the absence or presence of different concentrations of CMP5. The assay was conducted according to the manufacturer's instructions.

4.10 Immunofluorescence confocal microscopy

FLK-BLV cells were grown on coverslips with or without CMP5 treatment. After 48 h, the cells were fixed with 4% paraformaldehyde for 15 min at room temperature; next, they were permeabilized with 0.5% Triton X for 5 min and then blocked with 5% skim milk for 30 min. The gp51 staining in the cell membrane was performed without the permeabilization step. The cells were incubated with anti-BLV gp51 Mab (BLV 2) (1:100; VMRD) or anti-BLV Gag Mab (BLV 3) (1:100; VMRD) for 1 h at room temperature followed by 30 min incubation with Alexa Fluor 488 rabbit anti-mouse for Gag or Alexa Fluor 594 rabbit anti-mouse for Env (1:300; Invitrogen, Carlsbad, CA, USA). Nuclei were stained with Hoechst 33342 (1:2000; ImmunoChemistry Technologies LLC. Bloomington, MN, USA) for 5 min in the dark. After each staining step, the samples were washed three times with PBS. The coverslips were mounted on glass slides and fluorescence images were obtained using an FV1000 confocal laser-scanning microscope (Olympus, Tokyo, Japan).

4.11 gp51 cell membrane staining by flow cytometry

FLK-BLV cells were washed twice with PBS, and 5×10^5 cells were stained with anti-BLV gp51 Mab (BLV 2) (1:50; VMRD) for 1 h on ice. The cells were then stained with APC rat anti-mouse (1:100; APC-anti mouse, BD Pharmingen, Franklin Lakes, NJ, USA) for 30 min on ice. Propidium Iodide (PI) was used for live/dead staining. Stained cells were analyzed using a BD AccuriTM C6 Plus with a sampler flow cytometer (BD Biosciences,

Franklin Lakes, NJ, USA). The data were analyzed using FlowJo v10 (FlowJo, LLC, Ashland, OR, USA).

4.12 Luminescence syncytium induction assay (LuSIA)

The LuSIA using CC81-GREMG cells was performed as described previously [127]. CC81 GREMG (1×10^5 cells) were co-cultured with 5×10^4 FLK-BLV cells in a 12-well plate in LuSIA medium, after which the indicated concentrations of CMP5 were added. After 48 h incubation, the cells were washed with phosphate-buffered saline and fixed with 4% formaldehyde/phosphate-buffered saline containing 10 μg/mL Hoechst 33342 (Thermo Fisher Scientific). The fluorescent syncytia were visualized by EVOS2 fluorescence microscopy (Thermo Fisher Scientific), and 9 fields of view in each well were automatically scanned with a 4× objective. Syncytia were detected by enhanced green fluorescent protein (EGFP) expression and counted using HCS Studio Cell Analysis software (Thermo Fisher Scientific).

4.13 Annexin V/7-AAD staining

KU-1 cells were seeded in a density of 1 x 10^6 cells/ml and treated with different concentrations of CMP5 for 24 h. After 24 h, the cells were collected and washed twice with PBS and once with 1X binding buffer, the cells were then resuspended with the 1X binding buffer at a concentration of 1 x 10^6 cells/ml. 1 x 10^5 cells were stained with 7-amino-actinomycin D (7-AAD) and Annexin V-PE (BD Biosciences) for 15 minutes at room temperature in the dark. Stained cells were analyzed using a BD AccuriTM C6 Plus with a sampler flow cytometer (BD Biosciences, Franklin Lakes, NJ, USA). Cells were considered to be early apoptotic if they were Annexin V +/ 7-AAD –, the double positive

population was considered to be in the late stage of apoptosis or dead cells.

4.14 Statistical analysis

All data were expressed as the mean ± standard deviation based on at least 3 independent experiments. Statistical significance was evaluated using Student's *t*-test. Differences were estimated to be significant at $p \leq 0.05$ (*) and strongly significant at $p \leq 0.01$ (**) and $p \leq 0.001$(***). The *p* value in animal experiments was calculated by Kruskal-Wallis test and Dunn's multiple comparisons test.

5 Results

5.1 PRMT5 is overexpressed in BLV-infected cattle with high PVL *in vivo*

BLV PVL is an important index of the risk of BLV transmission and infectivity as well as disease progression [12,44,45,47,50]. To investigate the correlation between PRMT5 expression and BLV PVL, we collected blood samples from 62 cows which were asymptomatic and had not developed symptoms of lymphoma at the time of blood collection. First, we performed the CoCoMo-qPCR-2 to calculate the BLV PVL, which was used to classify the cows into three groups: BLV-negative cattle (control group), BLV-infected cattle with a low-PVL (LPVL group), and BLV-infected cattle with a high-PVL (HPVL group). As described previously [46,69], the BLV-PVL equals to 10,000 copies/10^5 was set as a threshold to distinguish between HPVL and LPVL groups. Next, we evaluated PRMT5 expression at the RNA levels by qRT-PCR. The mean fold-change in PRMT5 was 1.12 ± 0.62 in the control group, 1.18 ± 0.64 in the LPVL group, and 1.64 ± 0.62 in the HPVL group (**Figure 7**A). PRMT5 expression was significantly higher in the HPVL group than in the uninfected group ($p = 0.0014$) and LPVL group ($p = 0.012$) (**Figure 7**A). Our results showed that PRMT5 was significantly overexpressed only in BLV-infected cattle with a high PVL but not in those with a low PVL. Furthermore, a positive correlation was obtained between the BLV PVL and the PRMT5 expression fold-change ($r = 0.52$) (**Figure 7**B).

5.2 PRMT5 overexpression starts from an early stage of BLV infection *in vivo*

As shown in **Figure 7**, PRMT5 was upregulated only in BLV-infected cattle with a high PVL. To further investigate the role of PRMT5 in BLV infection *in vivo*, we examined

whether PRMT5 is overexpressed in the early stage of BLV infection. Therefore, we performed experimental infection of five BLV-negative Japanese black calves carrying the susceptible alleles *BoLA-DRB3*1601/1601* which are related to a high PVL in BLV infection [128], and we collected blood samples at different time points during the first month of infection (0, 0.5, 1, 2, 3, and 4 weeks). Next, we monitored the BLV PVL and PRMT5 expression at each time point. The mean of BLV PVL was 0 copies/10^5 cells before infection (0 week), 34 copies/10^5 cells after 3 days, 1158 copies/10^5 cells after 1 week, 26,760 copies/10^5 cells after 2 weeks, 90,150 copies/10^5 cells after 3 weeks, and 62,440 copies/10^5 cells after 4 weeks (**Figure 8**A, line graph). The mean fold-change in PRMT5 was 1 before infection, 1.44 after 3 days, 1.48 after 1 week, 2.6 after 2 weeks, 3.7 after 3 weeks, and 2.3 after 4 weeks. The highest expression of PRMT5 was observed during the third week (fold-change = 3.74, $p = 0.0008$), and then the expression slightly decreased after 4 weeks (fold-change = 2.3, $p = 0.01$) (**Figure 8**B, bar graph). Interestingly and consistently with the data shown in **Figure 7**A, a strong positive correlation was found between fold-upregulation of PRMT5 and BLV PVL ($r = 0.79$) (**Figure 8**B). Thus, PRMT5 expression was upregulated in response to BLV infection, and the level of upregulation was positively correlated with the BLV PVL. Moreover, PRMT5 upregulation began in an early stage of BLV infection rather than being established after a long period of proviral latency.

5.3 PRMT5 overexpression continues to lymphoma stage of BLV infection *in vivo*

Finally, we investigated whether the change in PRMT5 expression in BLV-infected cattle occurred in the lymphoma stage of disease. We compared PRMT5 expression at the RNA level among 3 groups of cattle: 20 BLV-negative cattle, 42 BLV-infected but clinically normal cattle, and 20 BLV-infected cattle with lymphoma. The fold-change in PRMT5

expression was 1.12 ± 0.62 in BLV-negative cattle, 1.48 ± 0.66 in the asymptomatic group, and 2.45 ± 1.1 in the lymphoma group (**Figure 9**A). This strongly indicates that PRMT5 upregulation continues until the lymphoma stage of BLV. Additionally, we confirmed the positive correlation between BLV PVL and PRMT5 expression fold-change (**Figure 9**B) (r = 0.524).

5.4 PRMT1 is also upregulated in HPVL BLV infection

In order to examine whether PRMT5 is specifically upregulated in BLV infection or other PRMTs member might also be involved in the process. We analyzed the mRNA level of PRMT1, which is Type 1 PRMTs, in the 62 cows used to analyze mRNA of PRMT5, which were asymptomatic and had not developed symptoms of lymphoma. We determined that PRMT1 is also upregulated in HPVL-BLV infection (fold-change = 1.85±0.52 vs. 1.03±0.25 in BLV-negative and 1.17±0.35 in LPVL) (**Figure 10**A) and we also found that the PRMT1 expression fold-change is positively correlated with BLV-PVL (r = 0.71) (**Figure 10**B). This indicates that several PRMTs, but not only PRMT5, might be involved in developing a BLV infection profile with a high proviral load.

5.5 PRMT5 knockdown enhances BLV gene transcription *in vitro*

The data shown in Figures 6–8 suggest that PRMT5 overexpression contributes to developing BLV infection with a high proviral load, and may influence which infected cows progress from the asymptomatic stage to the lymphoma stage. Next, we examined the impact of PRMT5 inhibition on BLV infection *in vitro*. PRMT5 is a well-known regulator of gene transcription either by catalyzing symmetric dimethylarginine of histone proteins to generate repressive histone markers including H2AR3me2s, H3R8me2s, and H4R3me2s or by

methylation of nonhistone proteins such as transcription factors [129,130]. To investigate the effect of PRMT5 inhibition on BLV gene expression, we knocked down PRMT5 in two cell lines, FLK-BLV, a permanently BLV-infected cell line, and PK15-BLV, a stably transfected cell line with CMVΔU3-pBLV-IF2, by siRNA. Next, we measured the mRNA of two viral transcripts, *gag* which is produced by the un-spliced mRNA and *tax* which is produced by the double splicing event. We found that PRMT5 knockdown significantly enhanced *gag* and *tax* transcription levels. In the FLK-BLV cell line, the fold-change of *gag* was 1.3 ($p = 0.03$) and of *tax* was 1.33 ($p = 0.04$) (**Figure 11**A). In the PK15-BLV cell line, the fold-change of *gag* was 1.72 ($p = 0.01$) and of *tax* was 1.6 ($p = 0.0014$) (**Figure 11**B).

5.6 PRMT5 knockdown enhances BLV protein expression *in vitro*

To confirm the finding shown in **Figure 11** at the protein level, FLK-BLV or PK15-BLV were transfected with siRNA targeting PRMT5 or mock siRNA for 48 or 72 h, and then cell lysates were prepared and the expression levels of two viral proteins (Env gp51and Gag p24) were evaluated by Western blotting analysis with anti-BLV gp51 Mab or anti-BLV p24 Mab. We confirmed that siRNA-mediated inhibition of PRMT5 in FLK-BLV significantly enhanced intracellular Env expression ($p = 0.02$) (**Figure 12**A). Moreover, the expression of both of Env and Gag in PK15-BLV were significantly enhanced as a result of PRMT5 knockdown ($p = 0.05$ and 0.02 for Env and Gag, respectively) (**Figure 12**B). The bands corresponding to the unprocessed Gag were shown in **Figure 13**A and **Figure 13**B for FLK-BLV and PK15-BLV, respectively. These results show that there was no defect in Gag processing after PRMT5 knockdown.

5.7 PRMT5 knockdown does not impair gp51 expression at the cell membrane

In order to exclude that the observed accumulation of BLV proteins is caused by the impaired protein trafficking to the cell membrane, we measured the expression level of Env-gp51 in the cell membrane by flow cytometry. PK15-BLV cells were transfected with siRNA targeting PRMT5 or mock siRNA for 72 h. PRMT5 knockdown was confirmed by Western blotting analysis. The cell membrane expression of gp51 was measured using flow cytometry. Here, we determined that PRMT5 knockdown does not impair the gp51 expression at the cell membrane (**Figure 14**). We, thus, concluded that the observed upregulation of BLV viral proteins after PRMT5 knockdown is caused by a higher expression rate rather than an impaired protein trafficking.

5.8 Selective PRMT5 inhibitor enhances BLV protein expression and alters gp51 mobility over SDS-PAGE

Next, we examined the effect of a pharmacological PRMT5 inhibitor on BLV protein expression. We used a small molecular PRMT5 inhibitor (CMP5), which was described previously by Alinari et al. [121]. We examined the effect of CMP5 on FLK-BLV and PK15-BLV. FLK-BLV or PK15-BLV was cultured in fresh medium with or without 5, 10, or 20 μ M of CMP5 for 48 h. Cell lysates were prepared, and the viral protein expression levels of Env and Gag were evaluated by Western blotting analysis with anti-BLV gp51 Mab or anti-BLV p24 Mab. Consistently, CMP5 treatment enhanced the protein expression of both gp51 and p24 in a dose-dependent manner in FLK-BLV, showing significance at the concentration 20 μM (**Figure 15**A). In contrast, in PK15-BLV, BLV expression was not significantly affected (**Figure 15**B). The bands corresponding to the unprocessed Gag were shown in

Figure 13C and in **Figure 13**D for FLK-BLV and PK15-BLV, respectively. These results also revealed that there was no defect in Gag processing after CMP5 treatment.

Unexpectedly, we found that CMP5 treatment altered gp51 electrophoretic mobility in SDS-PAGE and formed gp51 with a higher apparent molecular weight than gp51 in untreated cells. The change in the apparent molecular weight was more evident at 20 μM (**Figure 15**A and **Figure 15**B). Thus, we further investigated the possible impact of this inhibitor on BLV envelope protein glycosylation.

5.9 Selective PRMT5 inhibitor alters gp51 glycosylation processing *in vitro*

N-Glycan structures are classified into three types: high mannose, hybrid, and complex types. All types share a common tri-mannosyl core (Man3GlcNAc2). However, they differ in the structure of the remaining branches [131,132]. The complex type of *N*-glycan typically runs slower in SDS-PAGE than the high mannose type. To further illustrate the effect of CMP5 treatment on gp51 electrophoretic mobility in SDS-PAGE, we examined whether the slow migration of gp51 in the presence of CMP5 resulted from an increase in the complex type of *N*-glycan. Therefore, we cultured FLK-BLV or PK15-BLV in the absence (CMP5–) or presence of 20 μM of CMP5 (CMP5+) for 48 h. Cell lysates of each cell line were collected and divided into three parts: one part was not treated (PNGase F−/Endo H−), the second part was treated with PNGase F (PNGase F+), and the third part was treated with Endo H (Endo H+). As illustrated in **Figure 16**, PNGase F removed all types of *N*-linked glycosylation from the glycoprotein: high mannose, hybrid, and complex. Additionally, PNGase F severs the bond between *N*-acetylglucosamine (GlcNAc) and asparagine (Asn), liberating the entire sugar chain and converting asparagine (Asn) to aspartic acid (Asp). In contrast, Endo H cleaves only the high mannose and hybrid types of *N*-glycans, and the

complex type remains resistant to Endo H deglycosylation. Endo H cleaves the bond between the two GlcNAc residues in the core region, leaving one GlcNAc still bound to the protein [133].

Consistent with the observation shown in **Figure 15**, we found that CMP5 treatment (CMP5+) altered the electrophoretic mobility of gp51, forming a higher apparent molecular weight smear of gp51 in both FLK-BLV and PK15-BLV (**Figure 17**A and **Figure 17**B, PNGase F−/Endo H−). PNGase F treatment led to the accumulation of an approximately 30-KDa product in both FLK-BLV and PK15-BLV (**Figure 17**A and **Figure 17**B, PNGase F+). This corresponds to the calculated molecular weight of the envelope peptidic core in the absence of any glycosylation of BLV gp51. Thus, after PNGase F, the change in the migration pattern of gp51 disappeared, indicating that CMP5 affects the gp51 glycosylation pattern. Additionally, endo H treatment in PK15-BLV showed that the complex type of *N*-glycan of gp51 may increase after CMP5 treatment (**Figure 17**B, Endo H+) whereas in FLK-BLV, the complex type did not appear to be affected (**Figure 17**A, Endo H+). Our results show that CMP5 treatment can alter gp51 glycosylation processing.

5.10 CMP5 treatment does not change Env expression at the plasma membrane

Next, we examined whether CMP5 treatment affects Gag or Env localization or Env expression at the cell membrane. FLK-BLV cells were grown on coverslips in the absence (CMP5 –) or presence of 20 µM of CMP5 (CMP5 +) for 48 h; Gag was stained with a green fluorescent marker, Env was stained with a red fluorescent marker, and DAPI was used to stain the nucleus. Gag and Env localization were evaluated by fluorescence confocal microscopy. The cellular membrane staining of gp51was performed without the permeabilization step, the intracellular staining was conducted after the permeabilization with

0.5% Triton X-100 for 5 min. We observed a large accumulation of Gag after CMP5 treatment (**Figure 18**A). Additionally, the intracellular Env protein accumulated near to the nucleus after the treatment (**Figure 18**B). In contrast, the cell membrane expression of gp51 was not severely affected as demonstrated by the fluorescence confocal microscopy (**Figure 18**C) and by flow cytometry (**Figure 18**D).

5.11 Selective PRMT5 inhibitor impedes BLV ENV-mediated syncytia formation *in vitro*

It has been shown previously that perturbation of the *N*-linked glycan structure of the HIV and HTLV-1 Env proteins affects syncytia formation [134,135]. Therefore, we examined the impact of the PRMT5 inhibitor CMP5 on the syncytium formation ability. We used a newly developed LuSIA to quantify the syncytia [45,127]. Because examining the syncytia formation ability of PK15-BLV cells was not possible because of the relatively longer time required for forming the syncytia, we only assessed the effect of CMP5 on syncytia formation using the FLK-BLV cell line. The LuSIA depends on a new reporter cell line (CC81-GREMG) stably transfected with a reporter plasmid in which the EGFP reporter gene is expressed under control of the glucocorticoid response element (GRE)-mutated LTR-U3 promoter and enables direct visualization of syncytia. CC81-GREMG expresses EGFP in response to BLV trans-activator p38tax expression and forms fluorescent syncytia when cultured with BLV-producing cells.

FLK-BLV cells were co-cultured with CC81-GREMG cell in the absence or presence of different concentrations of CMP5. Interestingly, CMP5 treatment negatively affected syncytia formation; this was detected by eye under a fluorescence microscope (**Figure 19**A) and by automated quantification showing that the syncytia counts were decreased in a dose-dependent manner, showing significance at concentrations of 10 µM ($p = 0.017$) and 20 µM

(p = 0.0002) (**Figure 19**B). In contrast, the total cell count during the assay remained unaffected (**Figure 19**C). In addition, the maximum used concentration of CMP5 (20 µM) did not severely affect the viability of FLK-BLV or CC81-GREMG (**Figure 19**D). These observations exclude the toxic effect of CMP5 on FLK-BLV or CC81-GREMG. Our results obtained by LuSIA using CC81-GREMG cells strongly suggest that PRMT5 regulates the induction of syncytia by BLV Env.

5.12 PRMT5 inhibitor enhances apoptosis and decreases cell proliferation of KU-1 cell line

It is well known that PRMT5 plays a role as an oncogene protein; also, PRMT5 upregulation was determined in several human cancers, including B and T cell lymphoma [136–138], metastatic melanoma [139], neuroblastoma and glioblastoma [140], ovarian cancer [141], breast cancer [142], and gastric cancer [143]. Moreover, PRMT5 upregulation was recently determined in HTLV-1-mediated T-cell transformation [122] and EBV driven B-cell transformation [121]. We have already showed that PRMT5 is overexpressed in BLV infected cattle in the lymphoma stage (**Figure 9**A). Finally, we investigated whether PRMT5 inhibition affects bovine lymphoid cells proliferation or apoptosis. We used KU-1 cell line, which is a bovine lymphoid cell line, we showed that PRMT5 inhibitor decreases cell proliferation and enhances apoptosis (**Figure 20**). However, further studies using more lymphoid cell lines and using BLV-negative cell lines are required to fully demonstrate the potential therapeutic effects of PRMT5 inhibitors in BLV-mediated lymphoma.

6 Discussion

BLV-mediated pathogenicity depends on a delicate balance between viral gene expression and certain host-related genetic and epigenetic events [2]. The mutation rate of BLV is relatively low [61] and spontaneous variations in the BLV genome have a limited impact on the biological properties of the virus [62]. Thus, host factors are thought to play crucial roles in determining the BLV infection profile. Herein, we investigated the role of the host protein PRMT5 in BLV infection *in vivo* and *in vitro*. Our study revealed four conclusions as follows. First, our data suggested that PRMT5 overexpression is involved in the development of BLV infection with a high proviral load, thus affecting which infected cows progress from the asymptomatic stage to the lymphoma stage, and that PRMT5 overexpression may serve as an index of disease progression *in vivo*. Second, we demonstrated that PRMT5 acts as a novel negative regulator of BLV protein expression *in vitro.* Knockdown PRMT5 or its inhibition with an inhibitor enhanced BLV gene expression at the RNA and protein levels in BLV-infected cell lines. Third, CMP5 inhibition of PRMT5 demonstrated that the gp51 glycosylation pattern was altered under CMP5 treatment among different BLV-producing cell lines, thereby decreasing BLV-induced syncytium formation mediated by Env glycosylation. Finally, we provide an evidence that PRMT5 inhibitor treatment can decrease the proliferation and induces the apoptosis of a bovine lymphoid cell line. Our findings provide insight into the role of PRMT5 in the BLV viral life cycle and for the development of new anti-BLV drugs.

In this study, we found that PRMT5 was significantly upregulated in BLV-infected cattle with HPVL (PVL >10,000 copies/10^5) but not in those with LPVL (PVL ≤10,000 copies/10^5) (**Figure 7**). This finding indicates that PRMT5 upregulation is related to transmission. Furthermore, this upregulation continued to the lymphoma stage (**Figure 9**). We also

performed experimental infection of five cattle carrying the susceptible alleles *BoLA-DRB3*1601/*1601*, which are associated with an increased risk of developing BLV infection with HPVL, and we confirmed that PRMT5 is upregulated in response to BLV infection (**Figure 8**A), and its level of upregulation was strongly correlated with BLV PVL (**Figure 8**B). Finally, we found that PRMT5 upregulation starts as early as two weeks post-infection (**Figure 8**A). This finding supports previous observations that PRMT5 expression increases at 4–8 days post-EBV infection [121]. Taken together, our data suggest that overexpression of PRMT5 contributes to the development and maintenance of BLV infection. Notably, PRMT5 was not the only PRMT member to be upregulated in BLV infection. PRMT1, which is Type I PRMT, was also upregulated (**Figure 10**A). Additionally, our data showed that the PRMT1 expression fold-change was correlated with BLV PVL (**Figure 10**B). This indicates that PRMT5 is not specifically upregulated, but rather overexpression of other PRMTs is involved in regulating the BLV proviral load.

Our present study demonstrates that PRMT5 negatively regulates BLV expression, as PRMT5 inhibition including siRNA-mediated PRMT5 knockdown and treatment with CMP5 enhanced BLV gene expression at the transcriptional and protein levels in BLV-expressing cell lines, indicating that PRMT5 had an additive inhibitory effect on BLV gene expression (**Figure 11** and **Figure 12**). This result is supported by previous data showing that shRNA-mediated reduction in PRMT5 protein levels or its inhibition by a small molecule inhibitor (CMP5) in HTLV-1-infected lymphocytes resulted in increased viral gene expression [122]. PRMT5 catalyzes symmetric dimethylation of arginine residues in several histone and non-histone proteins [129,144]. Therefore, PRMT5 may regulate BLV gene expression either via an epigenetic mechanism and by producing repressive histone marks or methylation of non-histone proteins such as transcription factors. Additionally, our findings suggest why BLV maintains a silent state within infected cells *in vivo*. This proviral latency represents a

strategy for avoiding the host immune system and consequently allows for tumor development. Thus, numerous studies have focused on identifying compounds capable of reversing BLV latency to enhance immune clearance of the virus; previous studies also revealed histone deacetylation and DNA hypermethylation as epigenetic modifications involved in BLV transcriptional repression [145–147]. Therefore, understanding the mechanism of how PRMT5 regulates BLV expression requires further analysis.

Alinari and co-workers [121] investigated the role of PRMT5 in EBV-induced B-cell transformation and developed a small-molecule PRMT5 inhibitor (CMP5) capable of blocking EBV-driven B-cell transformation without affecting normal B cells. Interestingly, we found that CMP5 treatment of FLK-BLV and PK15-BLV affects the glycosylation pattern of BLV gp51. This was further supported by the finding that CMP5 treatment enhanced the formation of complex or hybrid types of *N*-glycan over the high-mannose type. Therefore, following CMP5 treatment, gp51 traveled more slowly than untreated gp51 in SDS-PAGE. The effects of CMP5 on gp51 glycosylation processing involve a sophisticated process requiring a large number of enzymes and organelles, named as the glycosylation machinery. The glycosylation machinery is a group of enzymes, chaperones, transporters, sugar donors, and accessory molecules necessary to form a specific glycan structure [148]. Therefore, glycosylation is a highly regulated and dynamic process that is extremely sensitive to changes in components of the glycosylation machinery. The diversity of glycans depends on not only the expression levels of the molecules involved in glycan biosynthesis, including glycosyltransferases, but also on the interplay of all regulatory molecules involved in the process. This may affect both the number of glycans (macroheterogeneity) and nature of these glycan chains (microheterogeneity) [148]. Thus, CMP5 treatment may alter the expression levels of some components of the glycosylation machinery, thereby altering the gp51 glycosylation pattern.

Notably, the effect of CMP5 treatment on the gp51 glycosylation pattern differs between the two cell lines (FLK-BLV and PK15-BLV), which belong to different host species. In the PK15-BLV cell line, CMP5 treatment enhanced the formation of the complex type of *N*-glycan over the high mannose type and this form of *N*-glycan can be secreted and incorporated in the viral particles. In FLK-BLV, however, the results did not reveal that the irregular type of *N*-glycan resulted from CMP5 treatment. Similarly, a previous report clearly showed distinct differences in the glycosylation profiles of HIV-1 Env gp120 expressed in CHO which originated from hamster and 293T cells originated from human [149]. Therefore, this variation in different cell lines is expected, as the nature of *N*-linked glycans attached to a glycoprotein is determined not only by the peptide backbone of a protein but also by the cell in which it is expressed.

Although CMP5 affects the gp51 apparent molecular weight, siRNA knockdown of PRMT5 did not appear to induce the same effect (**Figure 21**). The reason why this difference arose between siRNA-mediated PRMT5 knockdown and CMP5 treatment was unclear, but there are two possibilities. First, the impact of CMP5 treatment on gp51 glycosylation may be non-specific, resulting from inhibition of other PRMTs protein rather than PRMT5. Second, gp51 glycosylation is a highly dynamic process that is highly influenced by the time and efficiency of PRMT5 inhibition and differs between pharmacological inhibition and knockdown inhibition. Considering that Alinari and co-workers [121] showed that CMP5 selectively blocks S2Me-H4R3 in JeKo cells, whereas it is inactive against PRMT1, PRMT4, and PRMT7 in cellular screening assays, CMP5 appears to be selective for PRMT5 over Type1 PRMTs. Additionally, the initial predicted binding interactions of CMP5 with their hPRMT5 model suggested that the pyridine ring of CMP5 forms a p-stacking interaction with the Phe327 residue, which is critical for directing PRMT5 to catalyze symmetric dimethylation of arginine, explaining the selectivity of CMP5 for type II PRMT5 not type I

PRMTs. They also performed RNA-seq of PRMT5-shRNA or CMP5 treatment in transformed LCLs (60A) cells and observed significant overlap between genes de-repressed by CMP5 and genes de-repressed by PRMT5-shRNA confirming the specificity of this compound. In contrast, we observed that CMP5 treatment increases the apparent molecular weight of gp51 at 20 μM but not at 5 or 10 μM (**Figure 15**B). Therefore, the extent and duration of PRMT5 inhibition in siRNA knockdown may be insufficient to affect the glycosylation processing of gp51. Further transcriptomic or proteomic studies are required to identify the differentially expressed genes and determine the biological processes altered by CMP5 treatment or PRMT5 knockdown.

Our study showed that CMP5 treatment impeded BLV-induced syncytium formation, which was measured by LuSIA [45,127]. However, CMP5 treatment did not impair the gp51 expression at the cell membrane (**Figure 18**C and **Figure 18**D). Seemingly, the intracellular expression of Env accumulated near to the nucleus after CMP5 treatment (Figure 8B). The reason of this phenomena and whether or not it is related to the observed reduction of the syncytia formation remain unclear. On the other hand, previous studies reported that the electrophoretic mobility of the surface subunit of HIV envelope (gp120) was decreased when gp120 was synthesized in the presence of castanospermine or 1-deoxynojirimycin (inhibitors of glucosidase I). Consequently, these inhibitors blocked HIV-1-induced syncytium formation and cytopathicity [135,150,151]. Therefore, incorrect glycosylation processing of gp120 may negatively affect HIV-1 induced syncytium formation. In addition, BLV SU-linked *N*-glycosylation appeared to regulate the syncytium-forming capacity *in vitro* [25,152]. Taken together, CMP5 treatment likely impedes BLV-induced syncytium formation by affecting gp51 glycosylation processing. Our results clearly showed that PRMT5 expression regulates the correct gp51 glycosylation processing thereby induces the fusion properties to establish an infection.

As summarized in Figure 22, our data suggest that PRMT5 expression is upregulated in BLV infection *in vivo* and this upregulation might be required for the development and maintenance of BLV infection by three ways: first, in the early stage of BLV infection PRMT5 overexpression is important to ensure the correct gp51 glycosylation and mediate cell fusion then enhance cell-to-cell transmission to establish an infection. Second, in the stage of after developing BLV infection, PRMT5 upregulation works as a negative regulator of BLV gene expression and is involved in the silencing strategy adopted by BLV *in vivo* to avoid the host immune response, and thus PRMT5 expression correlates with BLV proviral load, i.e., the number of infected cells, in the late stages of BLV infection. Third, in the final stages of BLV infection, PRMT5 expression is further increased in order to inhibit apoptosis and enhance the cell proliferation, which contribute to the development of lymphoma.

7 Conclusion

The present study provides the first report that investigates the PRMT5 role in BLV infection and reveals a novel function of a small molecular compound on BLV-gp51 glycosylation processing. We demonstrated four conclusions as follows: First, we found that PRMT5 is overexpressed only in BLV-infected cattle with a high proviral load, but not in those with a low proviral load and this upregulation continued to the lymphoma stage. This PRMT5 upregulation began in an early stage of BLV infection rather than after a long period of proviral latency. These results indicate that PRMT5 overexpression is involved in the development of BLV infection with a high proviral load, thus affecting which infected cows progress from the asymptomatic stage to the lymphoma stage, and that PRMT5 overexpression may serve as an index of disease progression *in vivo*. Second, we provide an evidence *in vitro* that PRMT5 works as a negative regulator of BLV gene expression and PRMT5 overexpression could be implicated in the silencing strategy adopted by BLV to escape from the host immune response and consequently increase BLV proviral load. Third, we proved *in vitro* that PRMT5 is important to ensure the correct glycosylation processing of gp51, thereby maintains the gp51 cell fusion function and the induces syncytium formation ability, this can increase the cell-to-cell transmission of the virus to establish the first stage of the infection. Finally, PRMT5 overexpression can suppress the apoptosis and induce cell proliferation, which contribute to development of lymphoma. Our findings provide insight into the role of PRMT5 in the BLV viral life cycle and for the development of new anti-BLV drugs.

8 Acknowledgement

Years of Ph.D. have passed and the journey has come to an end. I am now recalling every single moment of this journey with a tear and smile. After spending years of my life doing experiments, preparing seminars, writing reports, having discussions and publishing the findings, I reached that wonderful moment when I collected all my work and wrote this thesis. First and foremost, I would like to thank God for giving me the strength, knowledge, ability, and opportunity to undertake this research and complete it satisfactorily.
This work would not have been completed without help and support from many people. So, I am very glad to express my great thanks to them:

Firstly, I would like to express my sincere thanks to my supervisor **Prof. Yoko Aida** for her patience, inspiration, and motivation and for helping and supporting me not only in every step of my research but also in my daily life in Japan, starting from the first day of my coming to Japan when she picked me up at Narita airport until this moment of finalizing my thesis work.

I would like to thank the Japanese government MEXT scholarship for giving me a great opportunity to pursue my study in Japan.
I would like to thank Prof. Shin-nasoke Takeshima for the very useful advice throughout my project.
I would like to thank my academic advisors: Prof. Kazumi Nakano and Prof. Jun-Ichiro Inoue for providing guidance and feedback throughout my Ph.D. course.

I would like to thank Professor Koru Uchimaru Professor Teturo Matano, Professor Kazumi Nakano, and Professor Kei Sato for the useful advice and suggestions during my pre-defense and final defense presentations.

Many thanks to all postdocs, graduate students, and technicians of the viral infectious disease lab, without whom I would not have achieved this research, and special thanks to my dear friends and labmates: Mairepati Palati, Rania Hamada, Lanlan Bai, Lowela Siarot, Samy Metwally, and Ryosuke Matsuura.

From the bottom of my heart, I would like to say big and special thank you for my family in Syria. I cannot forget their support and empathy with me, their daily video calls, and their warm and supporting talks during my stay in Japan. I am forever indebted to my parents, sisters, and brothers for always being with me and giving me the warm love even we live in opposite sides of the world. My lovely sister, Marwa, you were always special in cheering me up! I wish you all the best in your life.

Finally, my husband Ahmad – I couldn't have done my Ph.D. without your patience, enduring love, daily support, and encouragement, special thanks to you. You were always sharing my wish to fulfill my goal of getting the Ph.D. Degree. Now I am very close to achieving our goal and I truly dedicate this work to you. We both had hard days because of our long-distance relationship. Now, I am so thrilled to become united and to establish our small family.

9 Figures and Tables

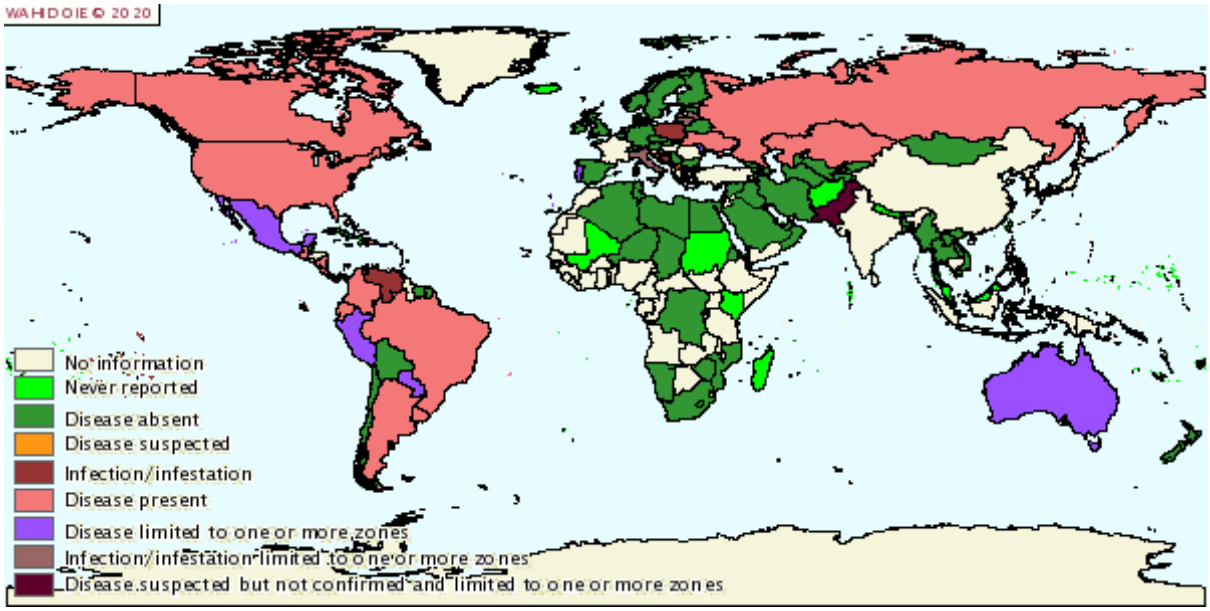

Figure 1. The worldwide prevalence of enzootic bovine leukosis. This figure is obtained from World Animal Health Information system (WAHIS) interface 2019. (https://www.oie.int/wahis_2/public/wahid.php/Diseaseinformation/Diseasedistributionmap?disease_type_hidden=&disease_id_hidden=&selected_disease_name_hidden=&disease_type=0&disease_id_terrestrial=35&species_t=0&disease_id_aquatic=999&species_a=0&sta_method=semesterly&selected_start_year=2019&selected_report_period=1&selected_start_month=1&date_submit=OK)

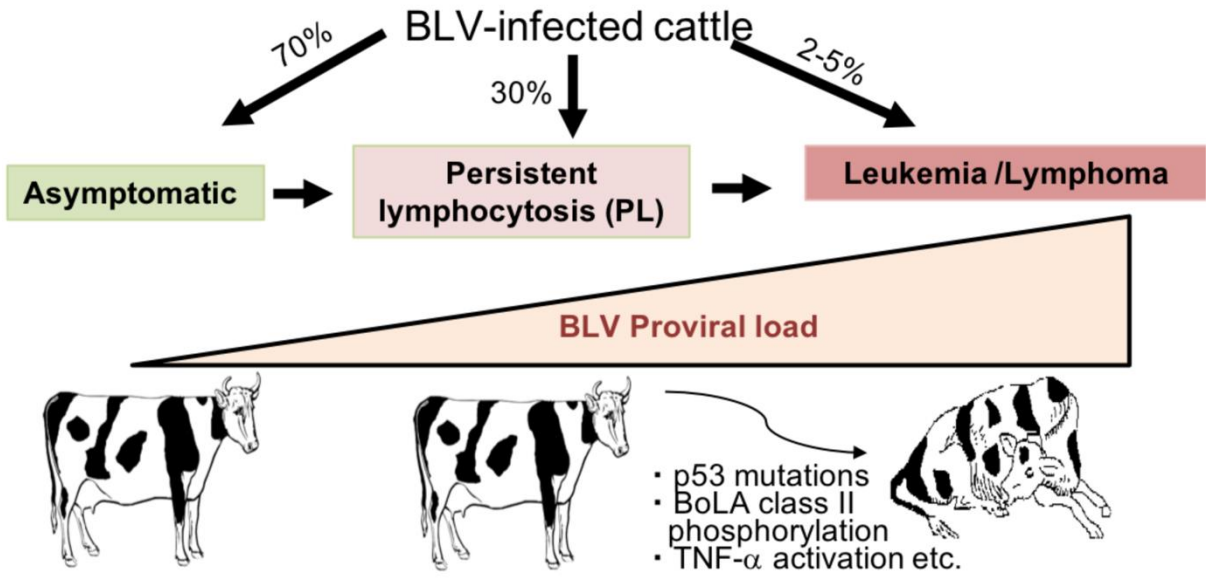

Figure 2. A schematic representation of disease progression in BLV-infected cattle

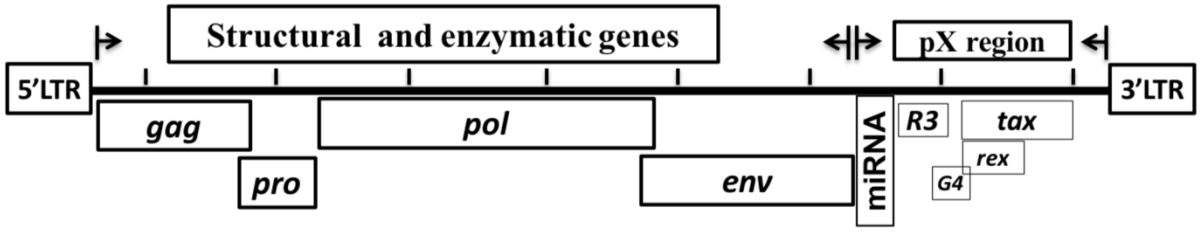

Figure 3. A schematic representation of BLV genome structure. BLV genome are flanked between two long terminal repeats. The structural and enzymatic gene encode for a protein required to form the viral particles, the pX region encodes regulatory proteins required for viral life cycle and pathogenicity

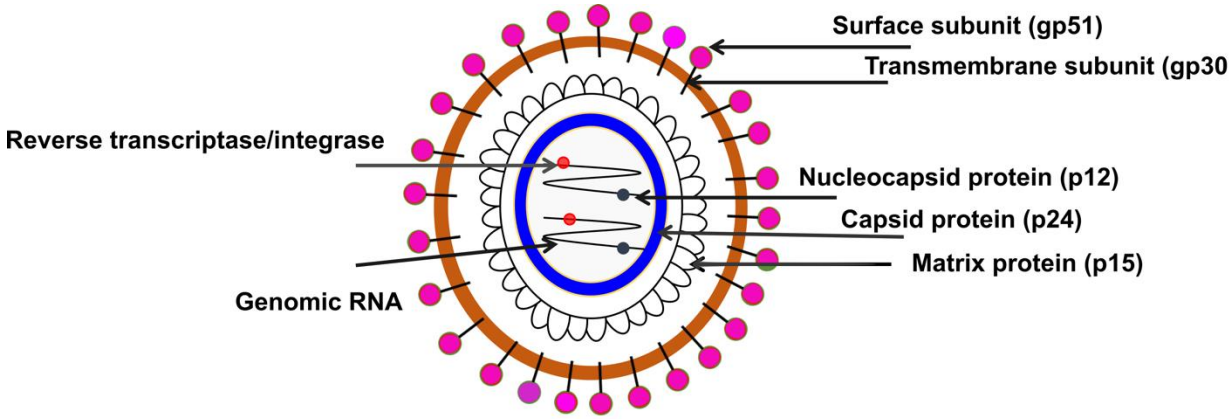

Figure 4. A schematic representation of BLV viral particles. Two copies of single stranded genomic RNA are packaged in a viral particle. The capsid is formed from the p24 protein and it contains the viral RNA interacting with nucleocapsid NC (p12). The capsid contains also two enzymatic proteins RT that is required for reverse transcription and IN that is required, for integration of the viral genome. The matrix protein MA (p15) connects the capsid with the envelope that is formed by a lipid bilayer of host cell and a complex of two viral proteins (gp51 SU and gp30 TM).

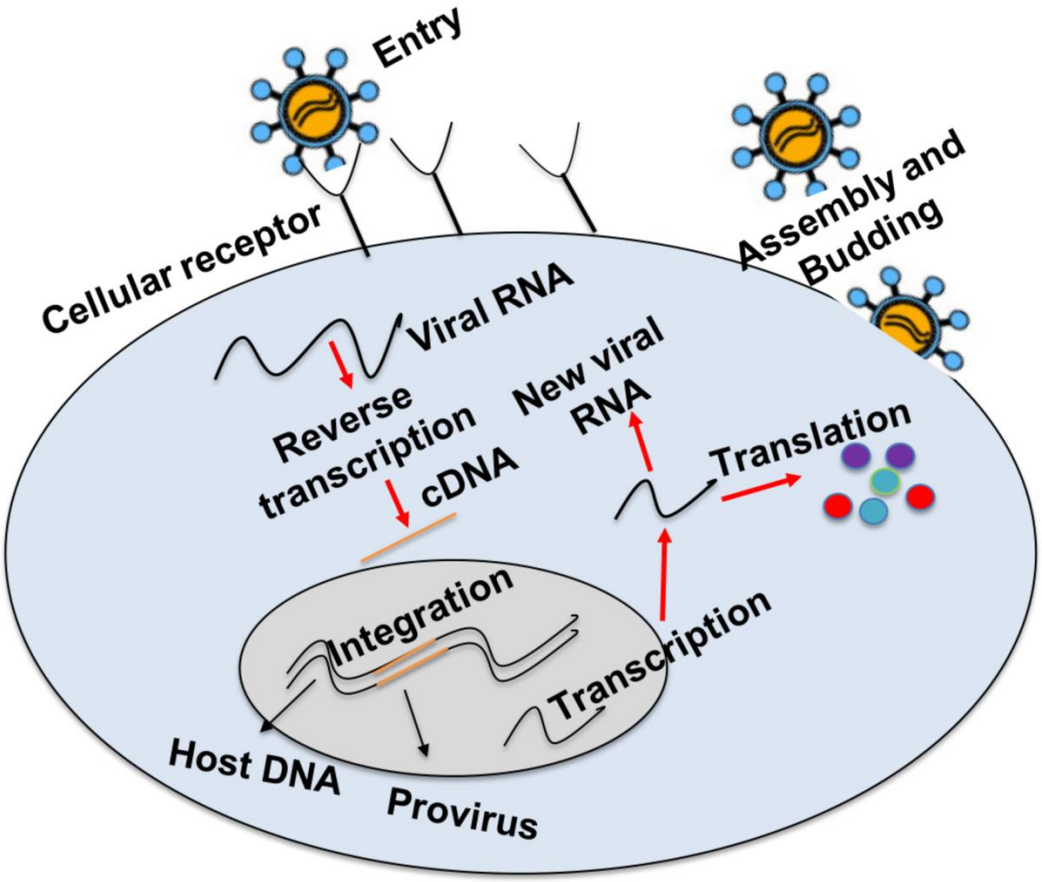

Figure 5. Infectious cycle of BLV replication. The infectious cycle of BLV replication includes: attachment of the gp51 of the virus to the target cell; fusion of virus and cellular membrane; viral uncoating and reverse transcription; proviral integration; transcription and protein synthesis; viral assembly and budding.

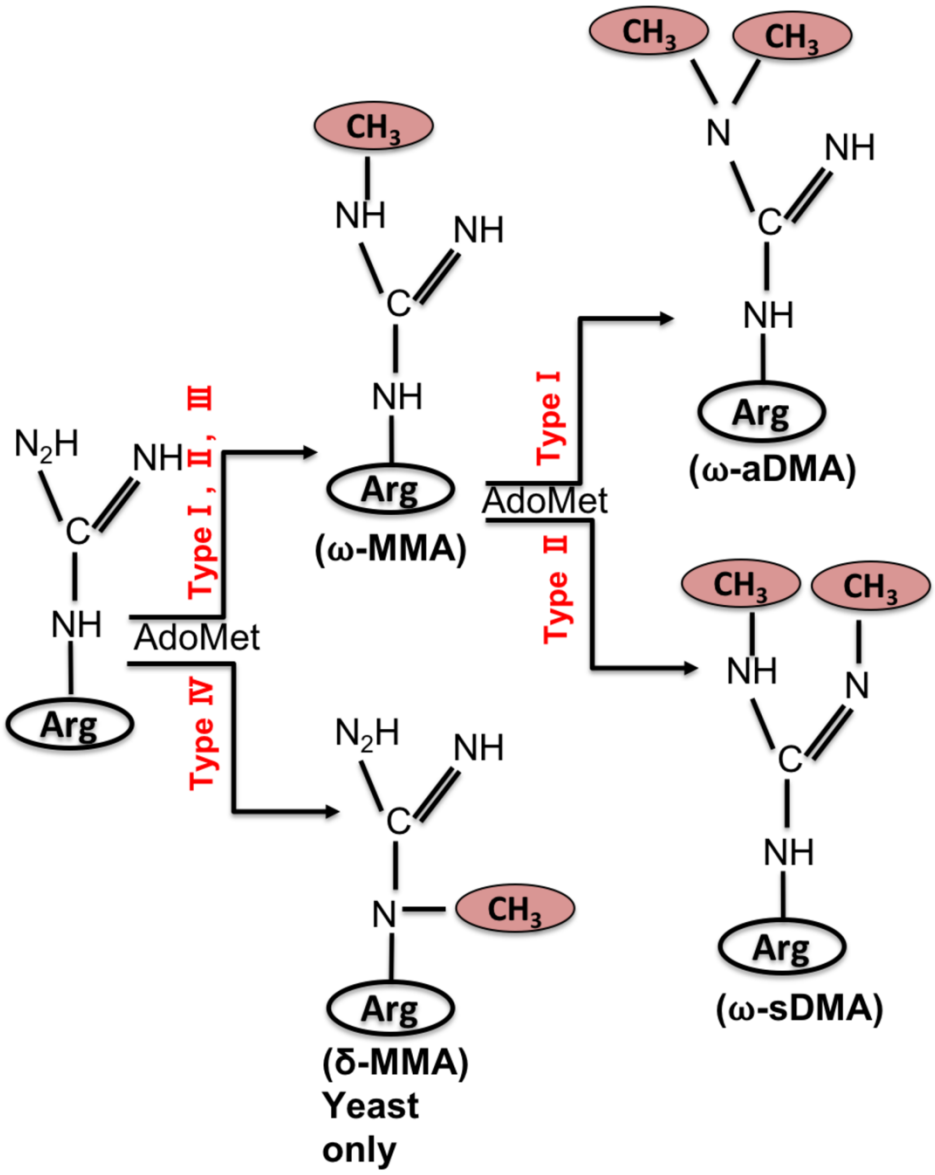

Figure 6. Types of protein arginine methyl transferase PRMTs.

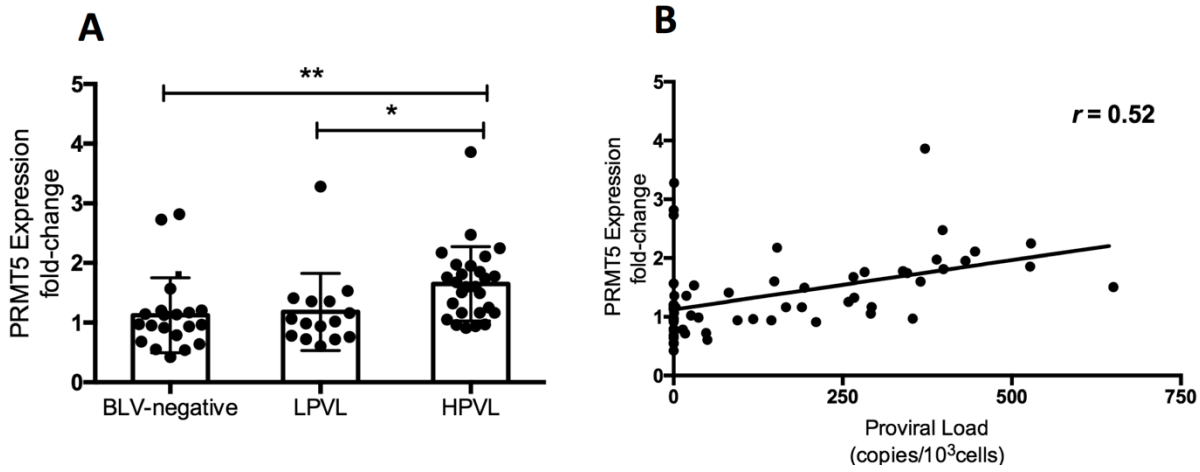

Figure 7. Change in PRMT5 expression at the RNA level in BLV infection. (A) PRMT5 expression at the RNA level of 20 BLV-negative cattle (PVL = 0), 15 BLV-infected but clinically normal cows with a low PVL (LPVL; PVL ≤ 10000 copies/10^5 cells), and 27 BLV-infected but clinically normal cows with a high PVL (HPVL; PVL >10000 copies/10^5 cells) was measured by qRT-PCR and the fold-change was calculated using the ΔΔCT method with normalization to GAPDH expression as an internal control. A scatter plot with bar showing the mean of PRMT5 expression fold-change in the three groups. BLV PVL was measured by CoCoMo-qPCR. Error bars represent the standard deviation of the biological replicates (20 BLV-negative, 15 LPVL, 27 HPLV). The *p* value was calculated using Kruskal-Wallis test (<0.0006). Dunn's multiple comparisons test was used to evaluate the significance between groups. The asterisk indicates a significant difference (*$p \leq 0.05$, **$p \leq 0.01$). **(B)** Correlation between BLV PVL of each cattle and the corresponding PRMT5 expression fold-change (62 in total), Spearman r was used to evaluate the strength of the correlation.

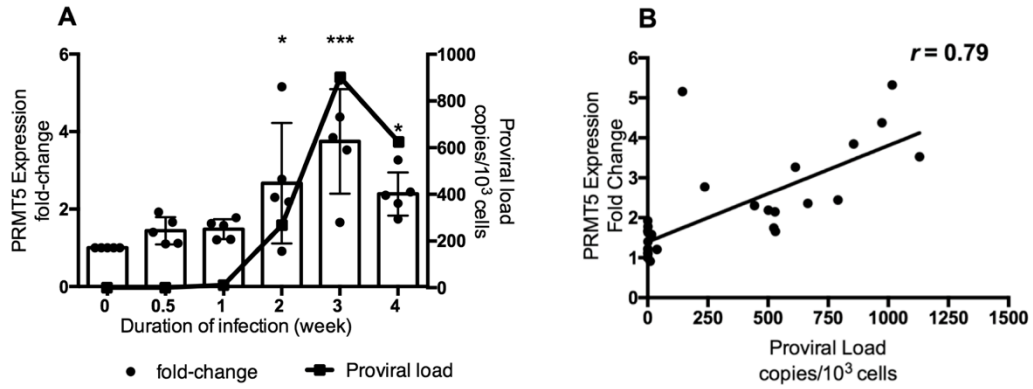

Figure 8. Change in PRMT5 expression at the RNA level in response to experimental BLV infection during the early stage of infection. **(A)** Five BLV-negative Japanese black calves carrying susceptible alleles *BoLA-DRB3*1601/*1601* were experimentally challenged intravenously with BLV, and RNA and DNA were extracted from these animals at six time points during the first month of infection. The BLV PVL was measured by CoCoMo-qPCR using genomic DNA. PRMT5 expression was measured by qRT-PCR using RNA, and the fold-change was calculated using the ΔΔCT method with normalization to GAPDH expression as an internal control. A combined bar and line graph show the mean of PRMT5 expression fold-change at each point (bar graph and left axis) with the corresponding mean of proviral load (line graph and right axis). Error bars represent the standard deviation of the PRMT5 fold-change of five cattle, *p* value was calculated using the Kruskal-Wallis test (0.002), and Dunn's multiple comparisons test was used to compare the mean of the PRMT5 fold-change at each time point of infection with the mean before infection. The asterisk indicates a significant difference (* $p \leq 0.05$ and *** $p \leq 0.001$). **(B)** Correlation between BLV PVL of each cattle at each time point and the corresponding PRMT5 expression fold-change, Spearman r was used to evaluate the strength of the correlation.

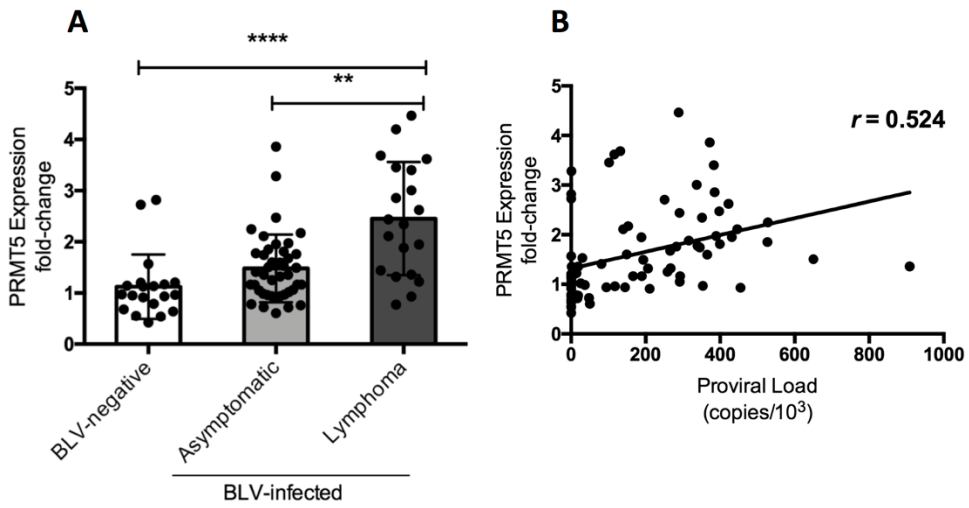

Figure 9. PRMT5 gene expression at the RNA level in BLV-infected cattle with lymphoma. (A) PRMT5 expression at the RNA level of 20 BLV-negative cattle, 42 BLV-infected but clinically normal cows, and 20 BLV-infected cattle with lymphoma was measured by qRT-PCR and the fold-change was calculated using the ΔΔCT method with normalization to GAPDH expression as an internal control. A scatter plot with bar showing the mean of the fold-change in PRMT5 expression of the 3 groups of cattle. The *p* value was calculated using Kruskal-Wallis test (<0.0001), and Dunn's multiple comparisons test was used to evaluate the significance among groups. The asterisk indicates a significant difference (** $p \leq 0.001$ and **** $p \leq 0.0001$). **(B)** Correlation between BLV PVL of each cow and corresponding PRMT5 expression fold-change (81 in total), Spearman r was used to evaluate the strength of the correlation.

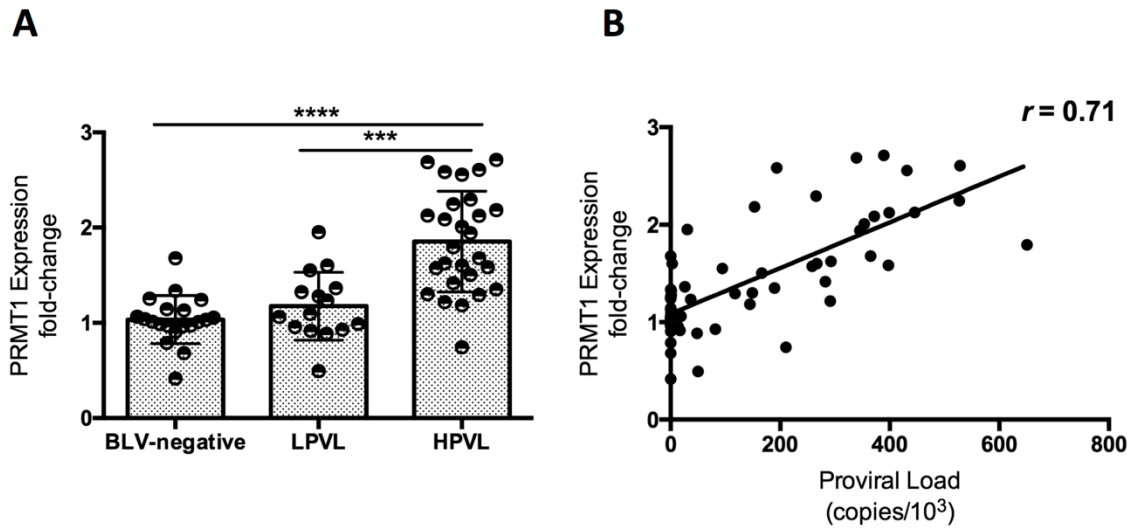

Figure 10. Change in PRMT1 expression at the RNA level in BLV infection. (A) PRMT5 expression at the RNA level of 20 BLV-negative cattle (PVL = 0), 15 BLV-infected but clinically normal cows with a low PVL (LPVL; PVL ≤ 10000 copies/10^5 cells), and 27 BLV-infected but clinically normal cows with a high PVL (HPVL; PVL >10000 copies/10^5 cells) was measured by qRT-PCR and the fold-change was calculated using the ΔΔCT method with normalization to GAPDH expression as an internal control. A scatter plot with bar showing the mean of PRMT5 expression fold-change in the three groups. BLV PVL was measured by CoCoMo-qPCR. Error bars represent the standard deviation of the biological replicates (20 BLV-negative, 15 LPVL, 27 HPLV). The *p* value was calculated using Kruskal-Wallis test (<0.0001). Dunn's multiple comparisons test was used to evaluate the significance between groups. The asterisk indicates a significant difference (***$p \leq$ 0.001, ****$p \leq 0.0001$). **(B)** Correlation between BLV PVL of each cattle and the corresponding PRMT5 expression fold-change (62 in total), Spearman r was used to evaluate the strength of the correlation.

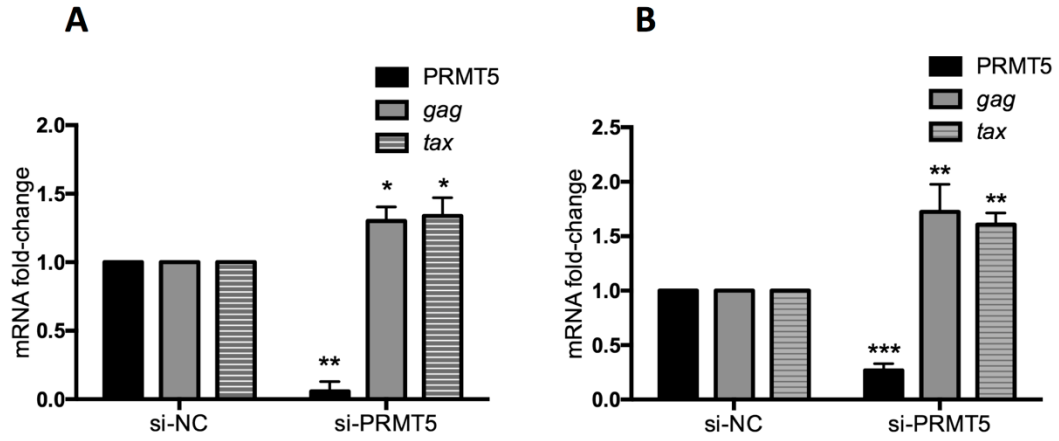

Figure 11. Effect of PRMT5 knockdown on BLV gene transcription. FLK-BLV **(A)** or PK15-BLV **(B)** cells were transfected with scramble siRNA (si-NC) or siRNA targeting PRMT5 (si-PRMT5) for 48 h for FLK-BLV or 72 h for PK15-BLV. BLV gene transcription (mRNA-*gag* and mRNA-*tax*) in addition to PRMT5 gene expression at the RNA level was evaluated by qRT-PCR. The ΔΔCT method was used to calculate the fold-change, and GAPDH expression was used as an internal control. Error bars represent the standard deviation of three experiments. The *p* value was calculated using the Student's *t*-test. The asterisk indicates a significant difference (*$p \leq 0.05$, ** $p \leq 0.01$ and *** $p \leq 0.001$).

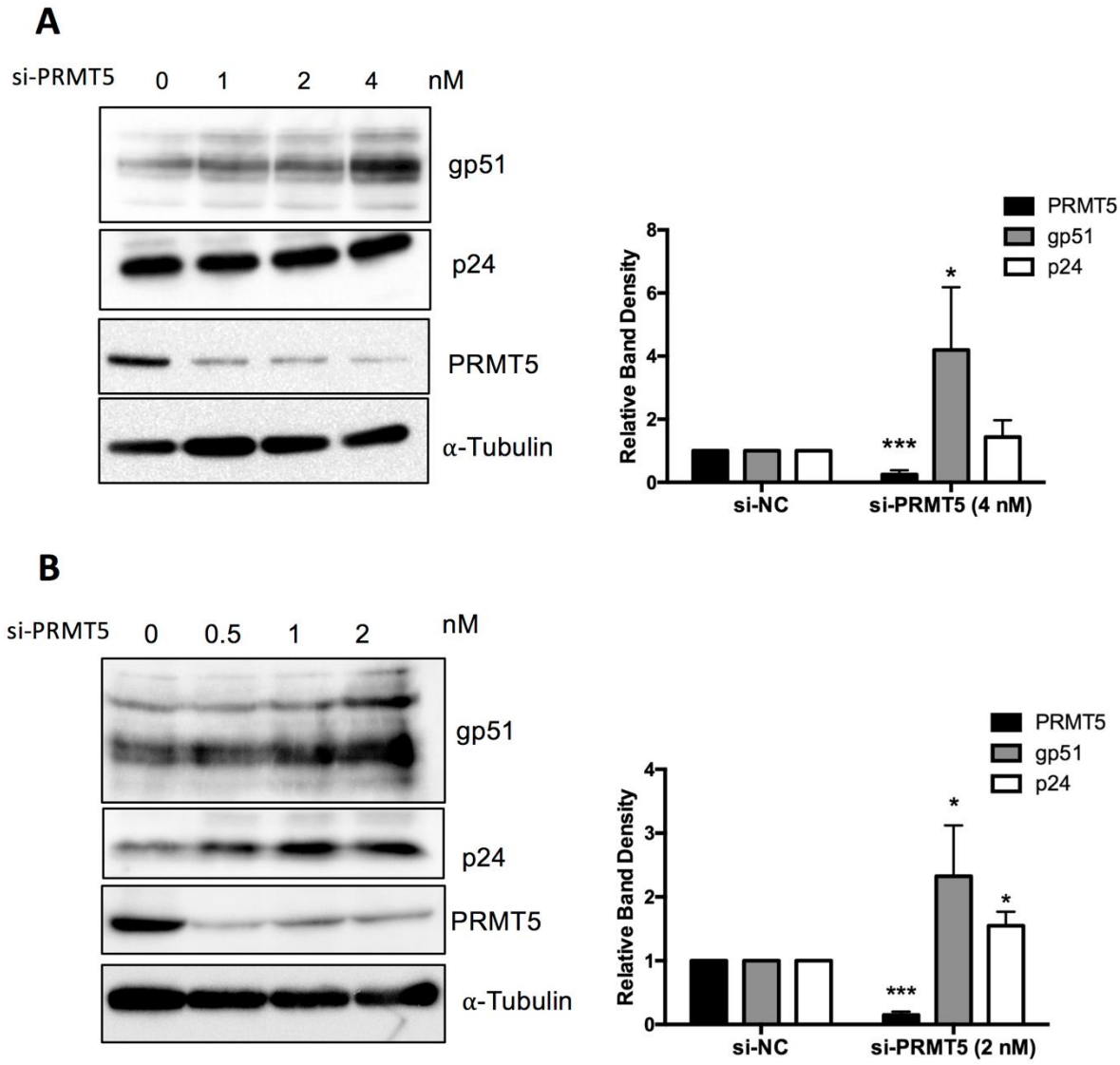

Figure 12. Effect of PRMT5 knockdown on BLV protein expression. FLK-BLV (**A**) or PK15-BLV (**B**) cells were transfected with scramble siRNA (si-NC) or siRNA targeting PRMT5 (si-PRMT5) at the indicated concentrations for 48 h for FLK-BLV or 72 h for PK15-BLV. Cell lysates were prepared, and the expression of two viral proteins (Env gp51 and Gag p24) were assessed by Western blotting analysis. Knockdown efficiency was evaluated by evaluating PRMT5 protein expression by Western blotting analysis. The relative band density of each protein normalized to α-tubulin expression is shown for each cell line. Error bars represent the standard deviation of three experiments. The *p* value was calculated by Student's *t*-test. The asterisk indicates a significant difference (*$p \leq 0.05$, ** $p \leq 0.01$ and *** $p \leq 0.001$). Positions of BLV gp51 and p24, PRMT5, and α-tubulin proteins are indicated.

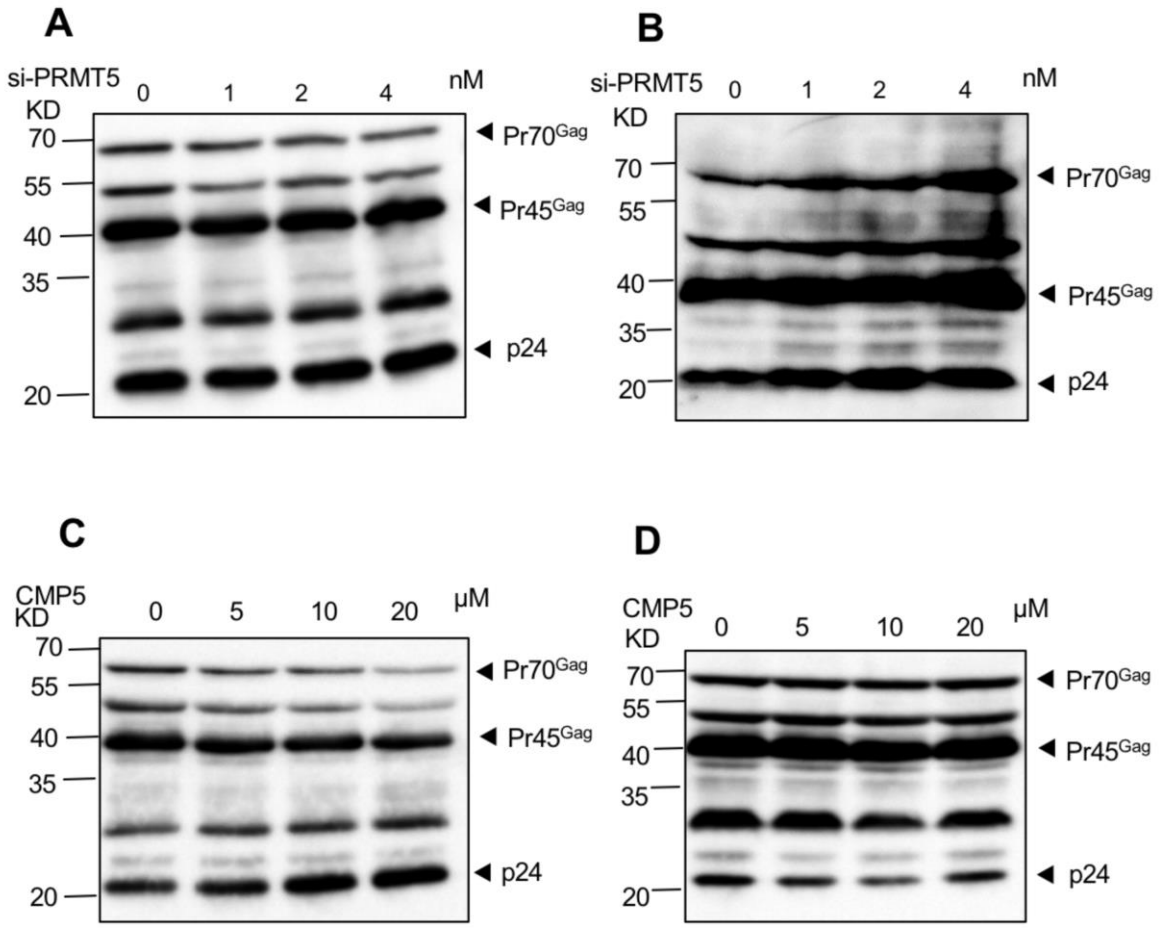

Figure 13. Effect of PRMT5 knockdown and CMP5 treatment on Gag processing. (A) Complete Western blotting image of Gag protein of data shown in Figure 12A. **(B)** Complete Western blotting image of Gag protein of data shown in Figure 12B. **(C)** Complete Western blotting image of Gag protein of data shown in Figure 15A. (D) Complete Western blotting image of Gag protein of data shown in Figure 15B. Positions of BLV p24, $Pr45^{Gag}$ and $Pr70^{Gag}$ are indicated.

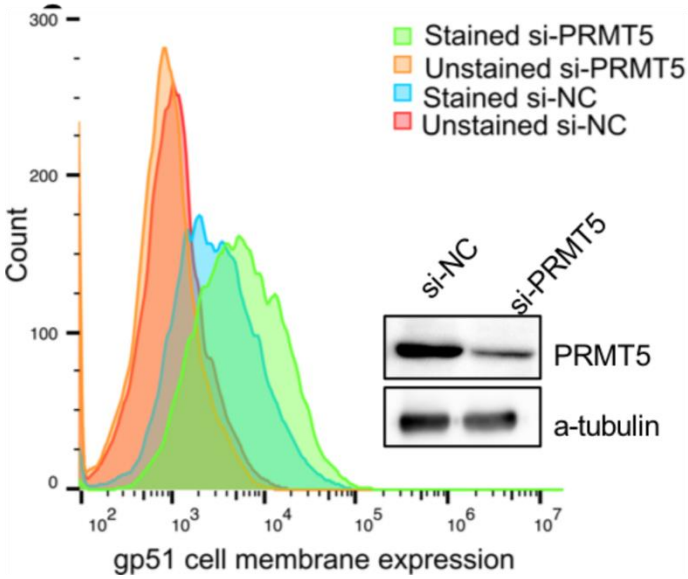

Figure 14. The effect of PRMT5 knockdown on gp51 cell membrane expression. PK15-BLV were transfected with scramble siRNA (si-NC) or siRNA targeting PRMT5 (si-PRMT5) for 72 h, the cells were collected, and gp51 cell membrane expression was assessed by flow cytometry.

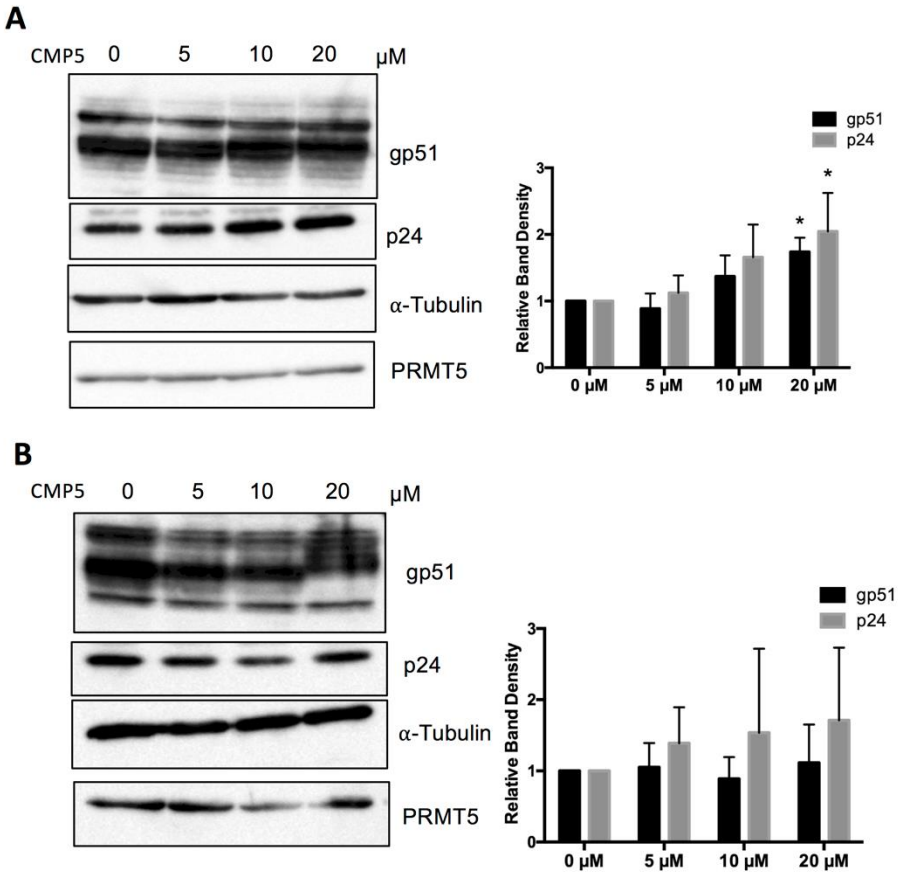

Figure 15. Effect of a small molecular PRMT5 inhibitor (CMP5) on BLV protein expression. FLK-BLV (**A**), or PK15-BLV (**B**) were cultured in the absence or the presence of the indicated concentrations of CMP5 for 48 h. Cell lysates were prepared, and viral proteins (Env gp51 and Gag p24) in addition to PRMT5 were evaluated by Western blotting. The relative band density of each protein normalized to α-tubulin expression is shown for each cell line. The PRMT5 expression level was not changed as a result of CMP5 treatment and was excluded from analysis. All band layers of gp51 were calculated. Error bars represent the standard deviation of three independent experiments. The *p* value was calculated using the Student's *t*-test. The asterisk indicates a significant difference (*$p \leq 0.05$). Positions of BLV gp51 and p24, PRMT5, and α-tubulin proteins are indicated.

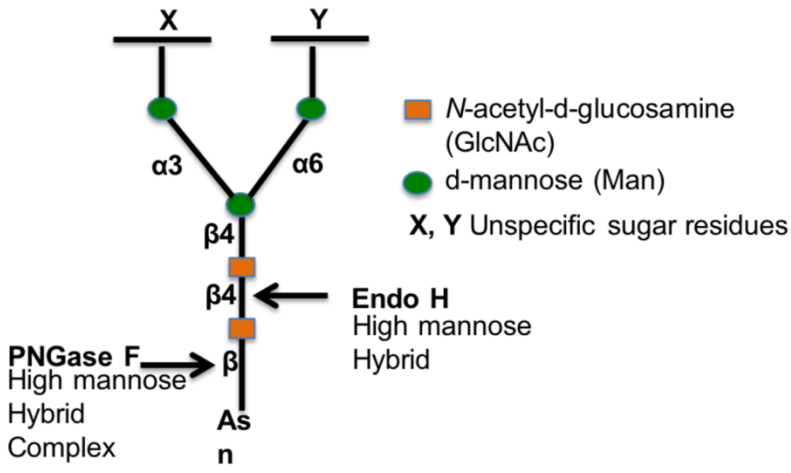

Figure 16. A schematic representation of PNGase F and Endo H sensitive bonds in the core of *N*-glycans.

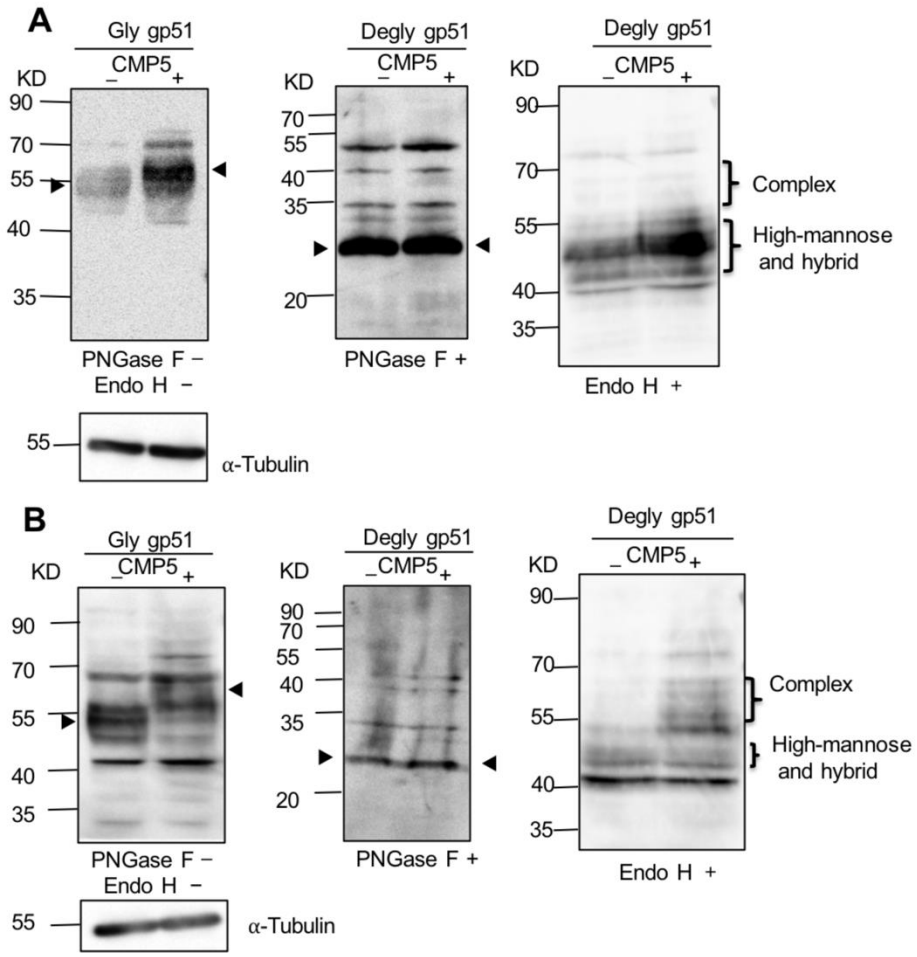

Figure 17. Deglycosylation assay of BLV gp51 using PNGase F and endo H. (A) FLK-BLV or **(B)** PK15-BLV were treated with Milli-Q water (CMP5−) or 20 µM CMP5 (CMP5+) for 48 h. Cell lysates were divided into three parts: one part was untreated (PNGase F−/Endo H−), the second part was deglycosylated by PNGase F (PNGase F+), and the third part was deglycosylated by Endo H (Endo H+). The cell lysates from the three conditions were subjected to Western blotting analysis with anti BLV gp51 (BLV2). α-Tubulin was used as a loading control. The positions of BLV gp51 protein with or without glycosylation, gp51 glycosylation pattern such as complex, and high-mannose and hybrid pattern, in addition to α-tubulin protein are indicated.

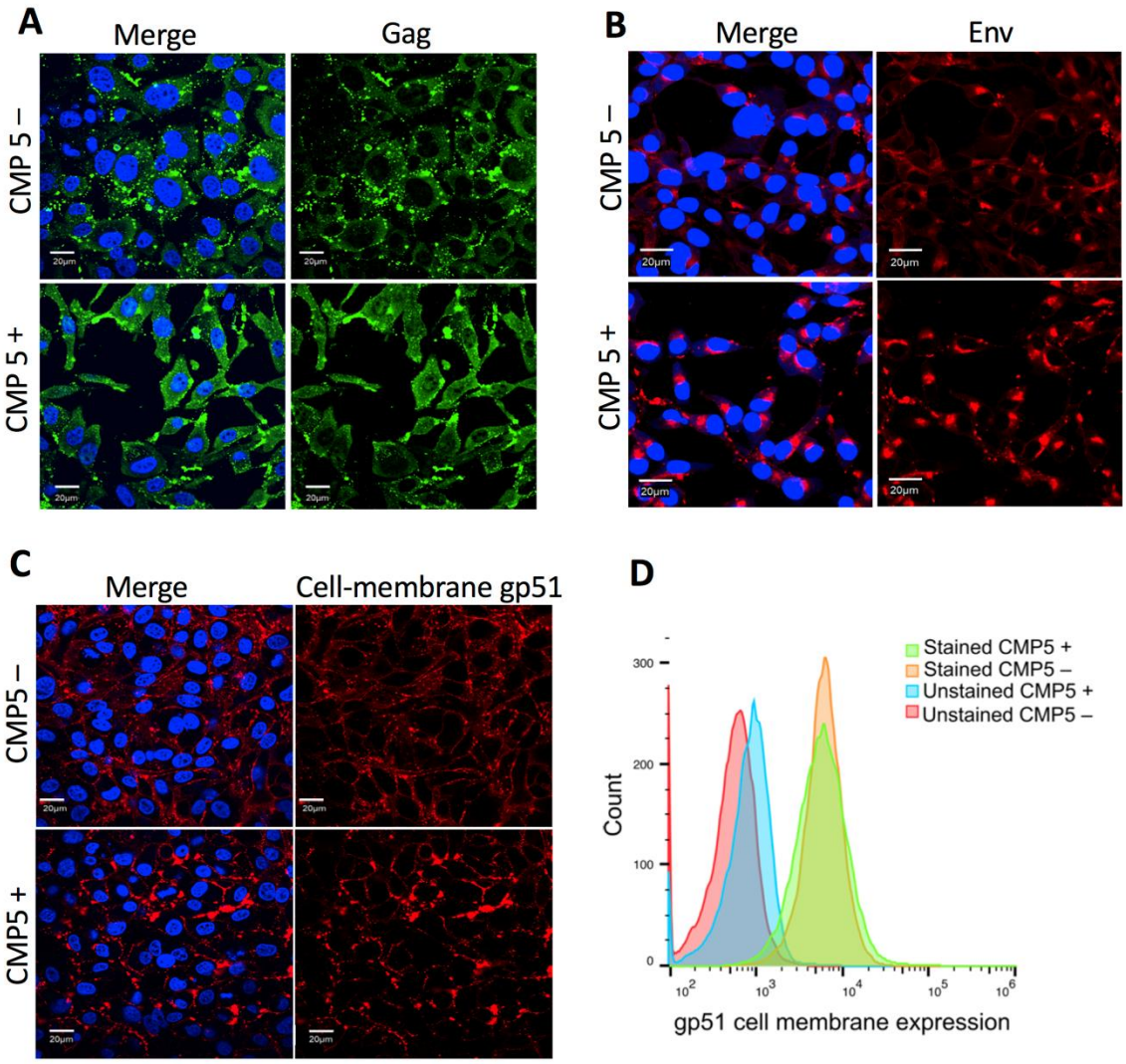

Figure 18. Effect of CMP5 on Gag and Env localization. (**A, B**) FLK-BLV were grown on coverslips and treated with Milli-Q water (CMP5 –) or CMP5 20 µM (CMP5 +), Gag was stained with green fluorescence (**A**), Env was stained with red fluorescence (**B**), The cellular membrane staining of gp51 was performed without the permeabilization step **(C)**. DAPI (blue fluorescence) was used to stain the nucleus, the merge picture represents Gag or Env with DAPI. The data is a representative of three experiments. Images were acquired with a 60X objective, and the scale bar is equal to 20 µm. (**D**) FLK-BLV were treated with Milli-Q water (CMP5 –) or CMP5 20 µM (CMP5 +), the cells were collected, and gp51 cell membrane expression was assessed by flow cytometry. The data is a representative of two experiments.

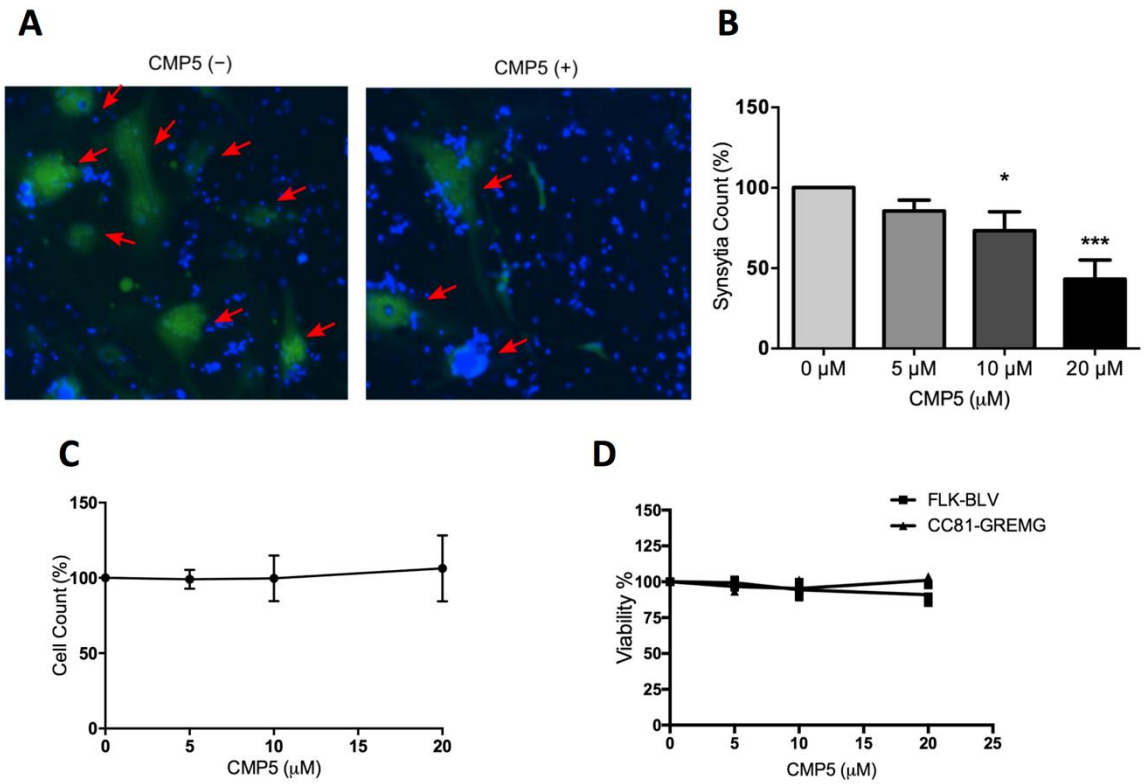

Figure 19. CMP5 effect on BLV ENV-mediated syncytia formation. A BLV-producing cell line FLK-BLV was co-cultured with a reporter cell line CC81-GREMG, and treated with Milli-Q water (CMP5−) or CMP5 at the indicated concentrations (CMP5+) for 48 h. **(A and B)**. Fluorescent syncytia in 9 fields of view in each well were automatically scanned by EVOS2 fluorescence microscopy with a 4× objective. Fluorescent syncytia were recognized by enhanced green fluorescent protein (EGFP) expression and gated by their area and intensity. Red arrows indicate positions of fluorescent syncytia. Hoechst 33342 was used to stain the nucleus. Each picture is a representative of 9 pictures acquired for each well. **(B)** Data analysis of (A) shows syncytia count using HCS Studio Cell Analysis software. Error bars represent the standard deviation of three independent experiments, *p* value was calculated by ANOVA (0.00031), Dunnett's multiple comparisons test showed a significant decrease in the syncytia count at 10 µM ($p = 0.017$) and 20 µM ($p = 0.0002$). **(C)** Effects of CMP5 on the total cell count taken from gating and counting of Hoechst 33342 staining using HCS Studio Cell Analysis software (Thermo Fisher Scientific). (**D**) CMP5 effect on cell viability according to WST-1 assay.

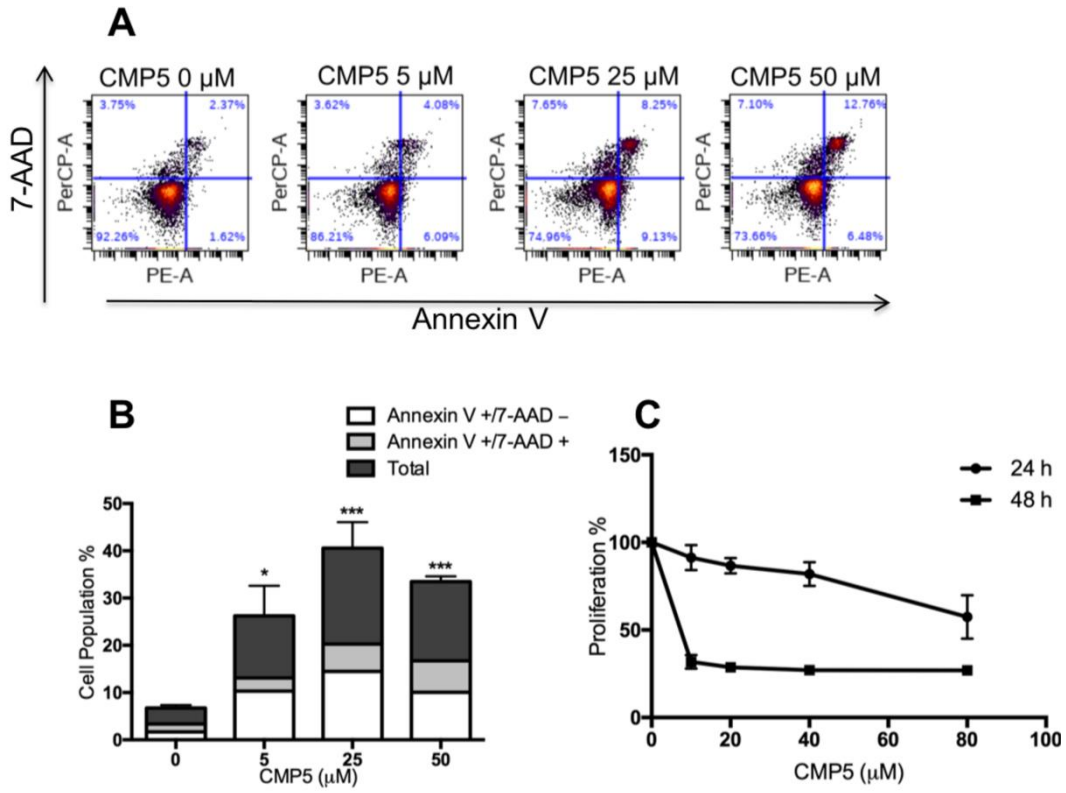

Figure 20. The effect of CMP5 treatment on Ku-1 proliferation and apoptosis. (A) KU-1 was treated with indicated concentration of CMP5, Annexin V/7-AAD staining was used to evaluate the apoptosis level. **(B)** Data analysis of (A). **(C)** The effect of CMP5 treatment on KU-1 prolifration using WST-1 assay.

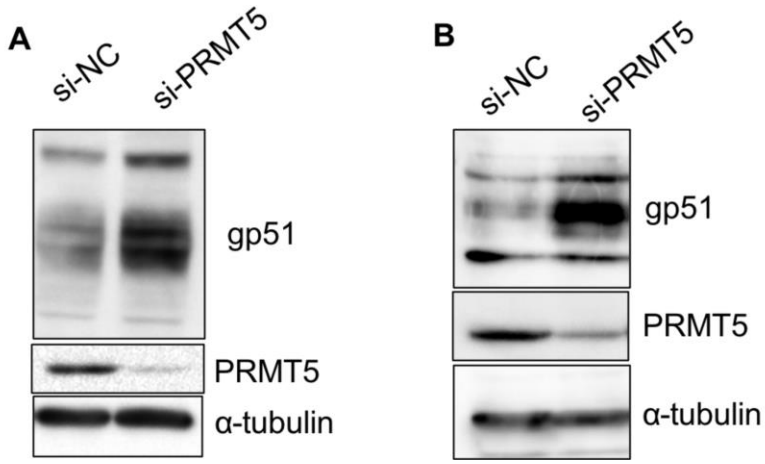

Figure 21. Effect of PRMT5 knockdown on gp51 electrophoretic mobility. (A) PRMT5 knockdown of FLK-BLV cell line using scramble siRNA (si-NC) or siRNA targeting PRMT5 (si-PRMT5) at 4 nM for 48 h. **(B)** PRMT5 knockdown of PK15-BLV cell line using scramble siRNA (si-NC) or siRNA targeting PRMT5 (si-PRMT5) at 2 nM.

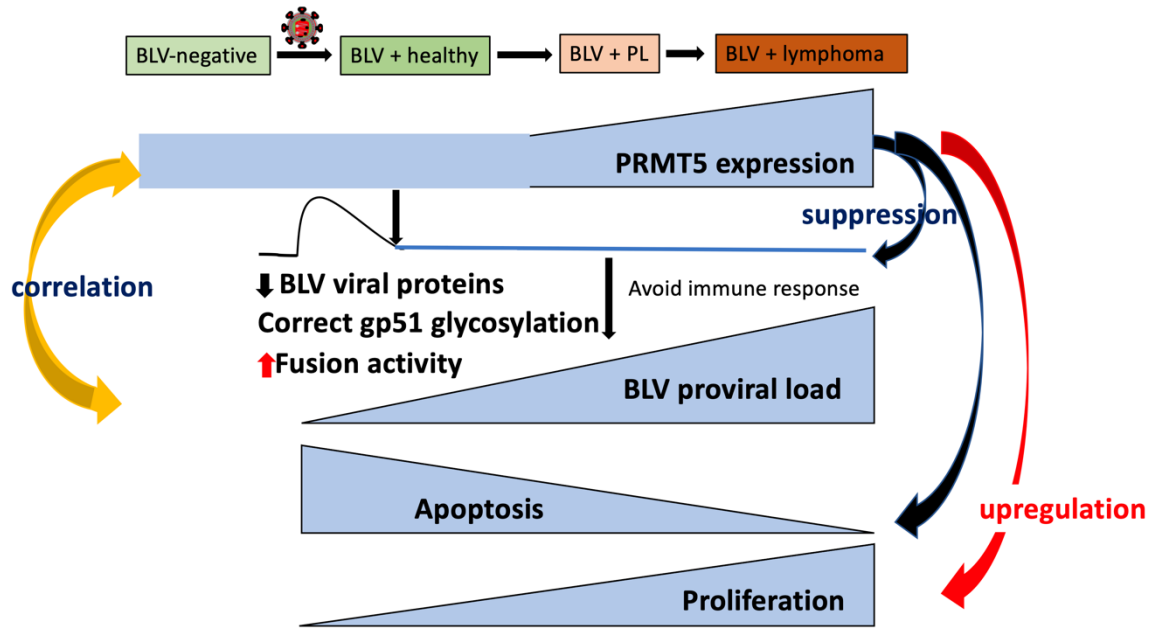

Figure 22. A hypothetical model for the roles of PRMT5 in development of BLV infection.

Table 1. The biological roles of PRMT5 in viruses' life cycle

Virus	PRMTs	Main findings	Reference
HTLV-1	PRMT5	▪ PRMT5 expression is upregulated during HTLV-1-mediated T-cell transformation ▪ PRMT5 inhibition enhances viral gene expression and decreases cellular proliferation	[122]
EBV	PRMT5	▪ PRMT5 is upregulated in response to EBV infection of germinal centre B cells ▪ EBV positive lymphomas and transformed cell lines have high expression of PRMT5 ▪ PRMT5 expression was limited to EBV-transformed cells, but not resting or activated B lymphocytes ▪ small-molecule PRMT5 inhibitor (CMP5) blocks EBV-driven B-lymphocyte transformation and survival while does not affect normal B cells	[153] [121]
HBV	PRMT5	▪ PRMT5 is an effective restrictor of HBV transcription and replication ▪ PRMT5-mediated H4R3me2s is a repressive marker of cccDNA transcription ▪ PRMT5 interferes with pregenomic RNA encapsidation by preventing its interaction with viral polymerase protein ▪ PRMT5 regulates HBV core protein (HBc) cell trafficking and function ▪ Overexpression of PRMT5 increases nuclear accumulation of HBc ▪ Down-regulation of PRMT5 results in reduced levels of HBc in nuclei of transfected cells	[123][124]
KSHV	PRMT5	▪ PRMT5 is a binding partner to the viral DNA processivity factor, ORF59 ▪ The expression of ORF59 competitively reduces the association of PRMT5 with COPR5, which lead to a reduction in PRMT5 mediated H4R3me2s and increase the active epigenetic mark, H3K4me3 marks, thereby the formation of the open chromatin required for transcription and DNA replication ▪ PRMT5 inhibition increases viral gene transcription	[125]
HIV-1	PRMT5	▪ PRMT5 is a Vpr-binding protein ▪ PRMT5 is critical to prevents Vpr degradation by the proteasome ▪ PRMT5 knockdown resulted in inefficient virus production	[126]

Table 2. Sample information of cattle BLV negative, BLV positive clinically normal, and BLV positive with lymphoma

Cattle ID	age (years)	breed	proviral lad copies/10^5 cells	Group
537	2.5	Holstein	0	BLV-negative
548	2.4	Holstein	0	BLV-negative
576	2	Holstein	0	BLV-negative
577	2	Holstein	0	BLV-negative
554	2.2	Holstein	0	BLV-negative
329	5.6	Holstein	0	BLV-negative
604	3.6	Holstein	0	BLV-negative
301	6	Holstein	0	BLV-negative
205	7.3	Holstein	0	BLV-negative
428	4.2	Holstein	0	BLV-negative
290	6.2	Holstein	0	BLV-negative
600	4	Holstein	0	BLV-negative
478	3.5	Holstein	0	BLV-negative
458	3.8	Holstein	0	BLV-negative
249	6.7	Holstein	0	BLV-negative
283	6.3	Holstein	0	BLV-negative
275	6.6	Holstein	0	BLV-negative
460	3.8	Holstein	0	BLV-negative
257	6.6	Holstein	0	BLV-negative
369	5.1	Holstein	0	BLV-negative
481	3.4	Holstein	54	LPVL
356	5.3	Holstein	3683	LPVL
177	7.8	Holstein	5011	LPVL
568	2.1	Holstein	84	LPVL

551	2.3	Holstein	90	LPVL
566	2.2	Holstein	306	LPVL
1069	5	Holstein	1882	LPVL
1301	3	Holstein	1355	LPVL
1388	2.4	Holstein	3026	LPVL
1405	2	Holstein	118	LPVL
845	8	Holstein	1704	LPVL
1357	3	Holstein	4801	LPVL
1394	2	Holstein	2587	LPVL
745	9	Holstein	9447	LPVL
1003	6	Holstein	8165	LPVL
324	5.7	Holstein	29139	HPVL
522	2.8	Holstein	26573	HPVL
30	10	Holstein	36525	HPVL
411	4.5	Holstein	18958	HPVL
445	3.9	Holstein	43142	HPVL
418	3.4	Holstein	52706	HPVL
295	6.1	Holstein	29271	HPVL
267	6.5	Holstein	21058	HPVL
211	7.3	Holstein	34544	HPVL
608	3.5	Holstein	28252	HPVL
349	5.4	Holstein	37174	HPVL
364	5.2	Holstein	14472	HPVL
561	2.2	Holstein	39759	HPVL
559	2.2	Holstein	38895	HPVL
371	5.1	Holstein	65026	HPVL

191	7.6	Holstein	26703	HPVL
384	5	Holstein	11753	HPVL
1092	5	Holstein	39911	HPVL
1113	5	Holstein	52828	HPVL
1237	4	Holstein	15294	HPVL
1298	3	Holstein	44567	HPVL
1402	2	Holstein	19345	HPVL
806	8	Holstein	25856	HPVL
852	8	Holstein	14907	HPVL
1084	5	Holstein	35351	HPVL
1289	3	Holstein	16634	HPVL
1400	2	Holstein	33916	HPVL
4	6	Holstein	11593	Lymphoma
6	11	Holstein	38316	Lymphoma
7	4	Holstein	31575	Lymphoma
9	5	Holstein	33691	Lymphoma
10	3	Holstein	18846	Lymphoma
11	7	Holstein	337714	Lymphoma
13	8	Holstein	20635	Lymphoma
17	6	Holstein	45448	Lymphoma
19	6	Holstein	1416	Lymphoma
20	6	Holstein	29065	Lymphoma
21	7	Holstein	28874	Lymphoma
22	4	Holstein	38527	Lymphoma
26	5	Holstein	13966	Lymphoma

27	7	Holstein	13182	Lymphoma
28	7	Holstein	35137	Lymphoma
29	5	Holstein	42230	Lymphoma
31	3	Holstein	90840	Lymphoma
33	4	Holstein	10221	Lymphoma
35	4	Holstein	1875	Lymphoma
39	5	Holstein	25072	Lymphoma

Table 3. Primer sequences for qRT-PCR used in the study

Gene	Forward 5´→3´	Reverse 5´→3´	Accession number
PRMT5 cattle	CCTGAATTGCGTCCCC GAAA	TGCAGAGGAAATCA AACCCCT	NM_001105374.1
PRMT5 FLK-BLV	TCCTCCATGTTCTGGA TGCG	GTGTGAGAAGTTGGT GCGT	XM_012181004.2
PRMT5 PK15-BLV	CCTGAATTGCGTCCCC GAAA	TGCAGAGGAAATCA AACCCCT	NM_001160093.1
Gag (p24)	GACCAAACGGCCCAT ATGAC	TTGGGCTGAGCTGAT TGTTG	DDBL: EF600696 [BLV] [Ref 67]
Tax	TGGAACAACTTAGTA ACGCATC	GCTCGCCTAGGGGTA GAATAC	DDBL: EF600696 [BLV] [Ref 67]
GAPDH cattle	TTCAACGGCACAGTCA AGG	ACATACTCAGCACCA GCATCAC	NM_001034034.2
GAPDH FLK-BLV	TGGTGAAGGTCGGAG TGAAC	ACGATGTCCACTTTG CCAGT	NM_001190390.1
GAPDH PK15-BLV	CTGAGACACGATGGT GAAGG	ACAATGTCCACTTTG CCAGA	NM_001206359.1

10 References

1. Gillet, N.; Florins, A.; Boxus, M.; Burteau, C.; Nigro, A.; Vandermeers, F.; Balon, H.; Bouzar, A.B.; Defoiche, J.; Burny, A.; et al. Mechanisms of leukemogenesis induced by bovine leukemia virus: Prospects for novel anti-retroviral therapies in human. *Retrovirology* **2007**, *4*, 1–32.
2. Aida, Y.; Murakami, H.; Takahashi, M.; Takeshima, S.N. Mechanisms of pathogenesis induced by bovine leukemia virus as a model for human T-cell leukemia virus. *Front. Microbiol.* **2013**, *4*, 1–11.
3. Onuma, M.; Honma, T.; Mikami, T.; Ichijo, S.; Konishi, T. Studies on the sporadic and enzootic forms of bovine leukosis. *J. Comp. Pathol.* **1979**, *89*, 159–167.
4. Polat, M.; Takeshima, S.N.; Aida, Y. Epidemiology and genetic diversity of bovine leukemia virus. *Virol. J.* 2017, *14*.
5. Ferrer, J.F.; Marshak, R.R.; Abt, D.A.; Kenyon, S.J. Persistent lymphocytosis in cattle: its cause, nature and relation to lymphosarcoma. *Ann. Rech. Vet.* **1978**, *9*, 851–857.
6. Burny, A.; Bex, F.; Bruck, C.; Cleuter, Y.; Dekegel, D.; Ghysdael, J.; Kettmann, R.; Leclercq, M.; Mammerickx, M.; Portetelle, D. Biochemical and epidemiological studies on bovine leukemia virus (BLV). *Hamatol. Bluttransfus.* **1979**, *23*, 445–452.
7. Nagaoka, Y.; Kabeya, H.; Onuma, M.; Kasai, N.; Okada, K.; Aida, Y. Ovine MHC class II DRB1 alleles associated with resistance or susceptibility to development of bovine leukemia virus-induced ovine lymphoma. *Cancer Res.* **1999**, *59*, 975–981.
8. Aida, Y.; Miyasaka, M.; Okada, K.; Onuma, M.; Kogure, S.; Suzuki, M.; Minoprio, P.; Levy, D.; Ikawa, Y. Further phenotypic characterization of target cells for bovine leukemia virus experimental infection in sheep. *Am. J. Vet. Res.* **1989**, *50*, 1946–51.
9. Aida, Y.; Okada, K.; Amanuma, H. Phenotype and Ontogeny of Cells Carrying a

Tumor-associated Antigen That Is Expressed on Bovine Leukemia Virus-induced Lymphosarcoma. *Cancer Res.* **1993**, *53*, 429–437.

10. Murakami, K.; Okada, K.; Ikawa, Y.; Aida, Y. Bovine leukemia virus induces CD5- B cell lymphoma in sheep despite temporarily increasing CD5+ B cells in asymptomatic stage. *Virology* **1994**, *202*, 458–465.
11. Kono, Y.; Sentsui, H.; Arai, K.; Ishida, H.; Irishio, W. Contact transmission of bovine leukemia virus under insect-free conditions. *Nippon juigaku zasshi. Japanese J. Vet. Sci.* **1983**, *45*, 799–802.
12. Watanuki, S.; Takeshima, S.N.; Borjigin, L.; Sato, H.; Bai, L.; Murakami, H.; Sato, R.; Ishizaki, H.; Matsumoto, Y.; Aida, Y. Visualizing bovine leukemia virus (BLV)-infected cells and measuring BLV proviral loads in the milk of BLV seropositive dams. *Vet. Res.* **2019**, *50*, 102.
13. Ferrer, J.F.; Piper, C.E. *AN EVALUATION OF THE ROLE OF MILK IN THE NATURAL TRANS-MISSION OF BLV. Annales de Recherches Vétérinaires*; 1978; Vol. 9;.
14. Hopkins, S.G.; DiGiacomo, R.F. Natural transmission of bovine leukemia virus in dairy and beef cattle. *Vet. Clin. North Am. Food Anim. Pract.* **1997**, *13*, 107–128.
15. Sagata, N.; Yasunaga, T.; Tsuzuku-Kawamura, J.; Ohishi, K.; Ogawa, Y.; Ikawa, Y. Complete nucleotide sequence of the genome of bovine leukemia virus: Its evolutionary relationship to other retroviruses. *Proc. Natl. Acad. Sci. U. S. A.* **1985**, *82*, 677–681.
16. de Brogniez, A.; Mast, J.; Willems, L. Determinants of the bovine leukemia virus envelope glycoproteins involved in infectivity, replication and pathogenesis. *Viruses* **2016**, *8*, 2–8.
17. Sagata, N.; Yasunaga, T.; Ohishi, K.; Tsuzuku-Kawamura, J.; Onuma, M.; Ikawa, Y.

Comparison of the entire genomes of bovine leukemia virus and human T-cell leukemia virus and characterization of their unidentified open reading frames. *EMBO J.* **1984**, *3*, 3231–3237.

18. Johnston, E.R.; Radke, K. The SU and TM envelope protein subunits of bovine leukemia virus are linked by disulfide bonds, both in cells and in virions. *J. Virol.* **2000**, *74*, 2930–5.
19. Zarkik, S.; Defrise-Quertain, F.; Portetelle, D.; Burny, A.; Ruysschaert, J.M. Fusion of bovine leukemia virus with target cells monitored by R18 fluorescence and PCR assays. *J. Virol.* **1997**, *71*, 738–740.
20. Bruck, C.; Mathot, S.; Portetelle, D.; Berte, C.; Franssen, J.D.; Herion, P.; Burny, A. Monoclonal antibodies define eight independent antigenic regions on the bovine leukemia virus (BLV) envelope glycoprotein gp51. *Virology* **1982**, *122*, 342–352.
21. Callebaut, I.; Vonèche, V.; Mager, A.; Fumière, O.; Krchnak, V.; Merza, M.; Zavada, J.; Mammerickx, M.; Burny, A.; Portetelle, D. Mapping of B-neutralizing and T-helper cell epitopes on the bovine leukemia virus external glycoprotein gp51. *J. Virol.* **1993**, *67*, 5321–5327.
22. Bai, L.; Otsuki, H.; Sato, H.; Kohara, J.; Isogai, E.; Takeshima, S. nosuke; Aida, Y. Identification and characterization of common B cell epitope in bovine leukemia virus via high-throughput peptide screening system in infected cattle. *Retrovirology* **2015**, *12*.
23. Bai, L.; Takeshima, S. nosuke; Isogai, E.; Kohara, J.; Aida, Y. Novel CD8+ cytotoxic T cell epitopes in bovine leukemia virus with cattle. *Vaccine* **2015**, *33*, 7194–7202.
24. Bai, L.; Takeshima, S.N.; Sato, M.; Davis, W.C.; Wada, S.; Kohara, J.; Aida, Y. Mapping of CD4+ T-cell epitopes in bovine leukemia virus from five cattle with differential susceptibilities to bovine leukemia virus disease progression. *Virol. J.*

2019, *16*.

25. de Brogniez, A.; Bouzar, A.B.; Jacques, J.-R.; Cosse, J.-P.; Gillet, N.; Callebaut, I.; Reichert, M.; Willems, L. Mutation of a Single Envelope N-Linked Glycosylation Site Enhances the Pathogenicity of Bovine Leukemia Virus. *J. Virol.* **2015**, *89*, 8945–8956.
26. VonecheSSll, V.; Callebaut, I.; Kettmann, R.; BrasseurSQS, R.; BurnySlIl, A.; PortetelleII, D. *THE JOURNAL OF BIOLOGICAL CHEMISTRY The 19-27 Amino Acid Segment of gp51 Adopts an Amphiphilic Structure and Plays a Key Role in the Fusion Events Induced by Bovine Leukemia Virus**; 1992; Vol. 267;.
27. Reth, M. Antigen receptor tail clue [5]. *Nature* 1989, *338*, 383–384.
28. Matsuura, R.; Inabe, K.; Otsuki, H.; Kurokawa, K.; Dohmae, N.; Aida, Y. Three YXXL sequences of a bovine leukemia virus transmembrane protein are independently required for fusion activity by controlling expression on the cell membrane. *Viruses* **2019**, *11*, 1–22.
29. Inabe, K.; Nishizawa, M.; Tajima, S.; Ikuta, K.; Aida, Y. The YXXL sequences of a transmembrane protein of bovine leukemia virus are required for viral entry and incorporation of viral envelope protein into virions. *J. Virol.* **1999**, *73*, 1293–301.
30. Bai, L.; Sato, H.; Kubo, Y.; Wada, S.; Aida, Y. CAT1/SLC7A1 acts as a cellular receptor for bovine leukemia virus infection. *FASEB J.* **2019**, fj201901528R.
31. Wallin, M.; Ekström, M.; Garoff, H. Receptor-Triggered but Alkylation-Arrested Env of Murine Leukemia Virus Reveals the Transmembrane Subunit in a Prehairpin Conformation. *J. Virol.* **2006**, *80*, 9921–9925.
32. Katoh, I.; Yoshinaka, Y.; Ikawa, Y. Bovine leukemia virus trans-activator p38tax activates heterologous promoters with a common sequence known as a cAMP-responsive element or the binding site of a cellular transcription factor ATF. *EMBO J.* **1989**, *8*, 497–503.

33. Willems, L.; Heremans, H.; Chen, G.; Portetelle, D.; Billiau, A.; Burny, A.; Kettmann, R. Cooperation between bovine leukaemia virus transactivator protein and Ha-ras oncogene product in cellular transformation. *EMBO J.* **1990**, *9*, 1577–1581.

34. Felber, B.K.; Derse, D.; Athanassopoulos, A.; Campbell, M.; Pavlakis, G.N. Cross-activation of the Rex proteins of HTLV-I and BLV and of the Rev protein of HIV-1 and nonreciprocal interactions with their RNA responsive elements. *New Biol.* **1989**, *1*, 318–328.

35. Willems, L.; Kerkhofs, P.; Dequiedt, F.; Portetelle, D.; Mammerickx, M.; Burny, A.; Kettmann, R. Attenuation of bovine leukemia virus by deletion of R3 and G4 open reading frames. *Proc. Natl. Acad. Sci. U. S. A.* **1994**, *91*, 11532–11536.

36. Florins, A.; Gillet, N.; Boxus, M.; Kerkhofs, P.; Kettmann, R.; Willems, L. Even Attenuated Bovine Leukemia Virus Proviruses Can Be Pathogenic in Sheep. *J. Virol.* **2007**, *81*, 10195–10200.

37. Lefèbvre, L.; Vanderplasschen, A.; Ciminale, V.; Heremans, H.; Dangoisse, O.; Jauniaux, J.-C.; Toussaint, J.-F.; Zelnik, V.; Burny, A.; Kettmann, R.; et al. Oncoviral Bovine Leukemia Virus G4 and Human T-Cell Leukemia Virus Type 1 p13II Accessory Proteins Interact with Farnesyl Pyrophosphate Synthetase. *J. Virol.* **2002**, *76*, 1400–1414.

38. Kincaid, R.P.; Sullivan, C.S. Virus-Encoded microRNAs: An Overview and a Look to the Future. *PLoS Pathog.* **2012**, *8*, e1003018.

39. Rosewick, N.; Momont, M.; Durkin, K.; Takeda, H.; Caiment, F.; Cleuter, Y.; Vernin, C.; Mortreux, F.; Wattel, E.; Burny, A.; et al. Deep sequencing reveals abundant noncanonical retroviral microRNAs in B-cell leukemia/lymphoma. *Proc. Natl. Acad. Sci. U. S. A.* **2013**, *110*, 2306–2311.

40. Gillet, N.A.; Hamaidia, M.; de Brogniez, A.; Gutiérrez, G.; Renotte, N.; Reichert, M.;

Trono, K.; Willems, L. Bovine Leukemia Virus Small Noncoding RNAs Are Functional Elements That Regulate Replication and Contribute to Oncogenesis In Vivo. *PLoS Pathog.* **2016**, *12*.

41. Katoh, I.; Yasunaga, T.; Yoshinaka, Y. Bovine leukemia virus RNA sequences involved in dimerization and specific gag protein binding: close relation to the packaging sites of avian, murine, and human retroviruses. *J. Virol.* **1993**, *67*, 1830–1839.
42. Mansky, L.M.; Krueger, A.E.; Temin, H.M. The bovine leukemia virus encapsidation signal is discontinuous and extends into the 5' end of the gag gene. *J. Virol.* **1995**, *69*, 3282–9.
43. Wang, H.; Norris, K.M.; Mansky, L.M. Involvement of the Matrix and Nucleocapsid Domains of the Bovine Leukemia Virus Gag Polyprotein Precursor in Viral RNA Packaging. *J. Virol.* **2003**, *77*, 9431–9438.
44. Jimba, M.; Takeshima, S.N.; Matoba, K.; Endoh, D.; Aida, Y. BLV-CoCoMo-qPCR: Quantitation of bovine leukemia virus proviral load using the CoCoMo algorithm. *Retrovirology* **2010**, *7*, 1–19.
45. Sato, H.; Watanuki, S.; Murakami, H.; Sato, R.; Ishizaki, H.; Aida, Y. Development of a luminescence syncytium induction assay (LuSIA) for easily detecting and quantitatively measuring bovine leukemia virus infection. *Arch. Virol.* **2018**, *163*, 1519–1530.
46. Lo, C.-W.; Borjigin, L.; Saito, S.; Fukunaga, K.; Saitou, E.; Okazaki, K.; Mizutani, T.; Wada, S.; Takeshima, S.; Aida, Y. BoLA-DRB3 Polymorphism is Associated with Differential Susceptibility to Bovine Leukemia Virus-Induced Lymphoma and Proviral Load. *Viruses* **2020**, *12*, 352.
47. Ohno, A.; Takeshima, S.N.; Matsumoto, Y.; Aida, Y. Risk factors associated with

increased bovine leukemia virus proviral load in infected cattle in Japan from 2012 to 2014. *Virus Res.* **2015**, *210*, 283–290.

48. Juliarena, M.A.; Gutierrez, S.E.; Ceriani, C. Determination of proviral load in bovine leukemia virus-infected cattle with and without lymphocytosis. *Am. J. Vet. Res.* **2007**, *68*, 1220–1225.

49. Takeshima, S.N.; Kitamura-Muramatsu, Y.; Yuan, Y.; Polat, M.; Saito, S.; Aida, Y. BLV-CoCoMo-qPCR-2: improvements to the BLV-CoCoMo-qPCR assay for bovine leukemia virus by reducing primer degeneracy and constructing an optimal standard curve. *Arch. Virol.* **2015**, *160*, 1325–1332.

50. Yuan, Y.; Kitamura-Muramatsu, Y.; Saito, S.; Ishizaki, H.; Nakano, M.; Haga, S.; Matoba, K.; Ohno, A.; Murakami, H.; Takeshima, S.N.; et al. Detection of the BLV provirus from nasal secretion and saliva samples using BLV-CoCoMo-qPCR-2: Comparison with blood samples from the same cattle. *Virus Res.* **2015**, *210*, 248–254.

51. Juliarena, M.A.; Barrios, C.N.; Ceriani, M.C.; Esteban, E.N. Hot topic: Bovine leukemia virus (BLV)-infected cows with low proviral load are not a source of infection for BLV-free cattle. *J. Dairy Sci.* **2016**, *99*.

52. Kettmann, R.; Deschamps, J.; Cleuter, Y. Leukemogenosis by bovine leukemia virus: Proviral DNA integration and lack of RNA expression of viral long terminal repeat and 3' proximate cellular sequences. *Proc. Natl. Acad. Sci. U. S. A.* **1982**, *79*, 2465–2469.

53. Lagarias, D.M.; Radke, K. Transcriptional activation of bovine leukemia virus in blood cells from experimentally infected, asymptomatic sheep with latent infections. *J Virol* **1989**, *63*, 2099–2107.

54. Tajima, S.; Tsukamoto, M.; Aida, Y. Latency of Viral Expression In Vivo Is Not Related to CpG Methylation in the U3 Region and Part of the R Region of the Long

Terminal Repeat of Bovine Leukemia Virus. *J. Virol.* **2003**, *77*, 4423–4430.

55. Tajima, S.; Aida, Y. Induction of expression of bovine leukemia virus (BLV) in blood taken from BLV-infected cows without removal of plasma. *Microbes Infect.* **2005**, *7*, 1211–1216.

56. Durkin, K.; Rosewick, N.; Artesi, M.; Hahaut, V.; Griebel, P.; Arsic, N.; Burny, A.; Georges, M.; Van den Broeke, A. Characterization of novel Bovine Leukemia Virus (BLV) antisense transcripts by deep sequencing reveals constitutive expression in tumors and transcriptional interaction with viral microRNAs. *Retrovirology* **2016**, *13*.

57. Rosewick, N.; Durkin, K.; Artesi, M.; Marçais, A.; Hahaut, V.; Griebel, P.; Arsic, N.; Avettand-Fenoel, V.; Burny, A.; Charlier, C.; et al. Cis-perturbation of cancer drivers by the HTLV-1/BLV proviruses is an early determinant of leukemogenesis. *Nat. Commun.* **2017**, *8*, 1–15.

58. Florins, A.; Gillet, N.; Asquith, B.; Boxus, M.; Burteau, C.; Twizere, J.C.; Urbain, P.; Vandermeers, F.; Debacq, C.; Sanchez-Alcaraz, M.T.; et al. Cell dynamics and immune response to BLV infection: A unifying model. *Front. Biosci.* **2007**, *12*, 1520–1531.

59. Pomier, C.; Alcaraz, M.T.S.; Debacq, C.; Lançon, A.; Kerkhofs, P.; Willems, L.; Wattel, E.; Mortreux, F. Early and transient reverse transcription during primary deltaretroviral infection of sheep. *Retrovirology* **2008**, *5*, 16.

60. Gillet, N.A.; Gutiérrez, G.; Rodriguez, S.M.; de Brogniez, A.; Renotte, N.; Alvarez, I.; Trono, K.; Willems, L. Massive Depletion of Bovine Leukemia Virus Proviral Clones Located in Genomic Transcriptionally Active Sites during Primary Infection. *PLoS Pathog.* **2013**, *9*, e1003687.

61. Mansky, L.M.; Temin, H.M. Lower mutation rate of bovine leukemia virus relative to that of spleen necrosis virus. *J. Virol.* **1994**, *68*, 494–499.

62. Murakami, H.; Uchiyama, J.; Suzuki, C.; Nikaido, S.; Shibuya, K.; Sato, R.; Maeda, Y.; Tomioka, M.; Takeshima, S. nosuke; Kato, H.; et al. Variations in the viral genome and biological properties of bovine leukemia virus wild-type strains. *Virus Res.* **2018**, *253*, 103–111.

63. Dequiedt, F.; Kettmann, R.; Burny, A.; Willems, L. Mutations in the p53 Tumor-Suppressor Gene Are Frequently Associated with Bovine Leukemia Virus-Induced Leukemogenesis in Cattle but Not in Sheep. *Virology* **1995**, *209*, 676–683.

64. Ishiguro, N.; Furuoka, H.; Matsui, T.; Horiuchi, M.; Shinagawa, M.; Asahina, M.; Okada, K. P53 Mutation As a Potential Cellular Factor for Tumor Development in Enzootic Bovine Leukosis. *Vet. Immunol. Immunopathol.* **1997**, *55*, 351–358.

65. Tajima, S.; Zhuang, W.Z.; Kato, M. V.; Okada, K.; Ikawa, Y.; Aida, Y. Function and conformation of wild-type p53 protein are influenced by mutations in bovine leukemia virus-induced B-cell lymphosarcoma. *Virology* **1998**, *243*, 235–246.

66. Komori, H.; Ishiguro, N.; Horiuchi, M.; Shinagawa, M.; Aida, Y. Predominant p53 mutations in enzootic bovine leukemic cell lines. *Vet. Immunol. Immunopathol.* **1996**, *52*, 53–63.

67. LEWIN, H.A.; BERNOCO, D. Evidence for BoLA-linked resistance and susceptibility to subclinical progression of bovine leukaemia virus infection. *Anim. Genet.* **1986**, *17*, 197–207.

68. Aida, Y.; Takeshima, S.; Baldwin C.L,; and kaushik A.K; *Bovine Immunogenetics, THE GENETICS OF CATTLE 2nd Edition*; (CAB international, pp 153-191,2014.

69. Takeshima, S.N.; Ohno, A.; Aida, Y. Bovine leukemia virus proviral load is more strongly associated with bovine major histocompatibility complex class II DRB3 polymorphism than with DQA1 polymorphism in Holstein cow in Japan. *Retrovirology* **2019**, *16*, 10–15.

70. Nikbakht Brujeni, G.; Ghorbanpour, R.; Esmailnejad, A. Association of BoLA-DRB3.2 Alleles with BLV Infection Profiles (Persistent Lymphocytosis/Lymphosarcoma) and Lymphocyte Subsets in Iranian Holstein Cattle. *Biochem. Genet.* **2016**, *54*, 194–207.

71. Brym, P.; Bojarojć-Nosowicz, B.; Oleński, K.; Hering, D.M.; Ruść, A.; Kaczmarczyk, E.; Kamiński, S. Genome-wide association study for host response to bovine leukemia virus in Holstein cows. *Vet. Immunol. Immunopathol.* **2016**, *175*, 24–35.

72. Takeshima, S.N.; Sasaki, S.; Meripet, P.; Sugimoto, Y.; Aida, Y. Single nucleotide polymorphisms in the bovine MHC region of Japanese Black cattle are associated with bovine leukemia virus proviral load. *Retrovirology* **2017**, *14*, 1–7.

73. Carignano, H.A.; Roldan, D.L.; Beribe, M.J.; Raschia, M.A.; Amadio, A.; Nani, J.P.; Gutierrez, G.; Alvarez, I.; Trono, K.; Poli, M.A.; et al. Genome-wide scan for commons SNPs affecting bovine leukemia virus infection level in dairy cattle. *BMC Genomics* **2018**, *19*, 1–15.

74. Hayashi, T.; Mekata, H.; Sekiguchi, S.; Kirino, Y.; Mitoma, S.; Honkawa, K.; Horii, Y.; Norimine, J. Cattle with the BoLA class II DRB3*0902 allele have significantly lower bovine leukemia proviral loads. *J. Vet. Med. Sci.* **2017**, *79*, 1552–1555.

75. Xu, A.; van Eijk, M.J.; Park, C.; Lewin, H.A. Polymorphism in BoLA-DRB3 exon 2 correlates with resistance to persistent lymphocytosis caused by bovine leukemia virus. *J. Immunol.* **1993**, *151*, 6977–85.

76. Konnai, S.; Usui, T.; Ikeda, M.; Kohara, J.; Hirata, T. ichi; Okada, K.; Ohashi, K.; Onuma, M. Tumor necrosis factor-alpha genetic polymorphism may contribute to progression of bovine leukemia virus-infection. *Microbes Infect.* **2006**, *8*, 2163–2171.

77. Guccione, E.; Richard, S. The regulation, functions and clinical relevance of arginine methylation. *Nat. Rev. Mol. Cell Biol.* **2019**, *20*, 642–657.

78. Bedford, M.T.; Richard, S. Arginine Methylation: An Emerging Regulator of Protein Function. *Mol. Cell* **2005**, *18*, 263–272.

79. Bedford, M.T. Arginine methylation at a glance. *J. Cell Sci.* **2007**, *120*, 4243–4246.

80. Pollack, B.P.; Kotenko, S. V.; He, W.; Izotova, L.S.; Barnoski, B.L.; Pestka, S. The human homologue of the yeast proteins Skb1 and Hs17p interacts with Jak kinases and contains protein methyltransferase activity. *J. Biol. Chem.* **1999**, *274*, 31531–31542.

81. Liu, F.; Zhao, X.; Perna, F.; Wang, L.; Koppikar, P.; Abdel-Wahab, O.; Harr, M.W.; Levine, R.L.; Xu, H.; Tefferi, A.; et al. JAK2V617F-Mediated Phosphorylation of PRMT5 Downregulates Its Methyltransferase Activity and Promotes Myeloproliferation. *Cancer Cell* **2011**, *19*, 283–294.

82. Sipos, A.; Iván, J.; Bécsi, B.; Darula, Z.; Tamás, I.; Horváth, D.; Medzihradszky, K.F.; Erdodi, F.; Lontay, B. Myosin phosphatase and RhoA-activated kinase modulate arginine methylation by the regulation of protein arginine methyltransferase 5 in hepatocellular carcinoma cells. *Sci. Rep.* **2017**, *7*, 1–15.

83. Lattouf, H.; Kassem, L.; Jacquemetton, J.; Choucair, A.; Poulard, C.; Trédan, O.; Corbo, L.; Diab-Assaf, M.; Hussein, N.; Treilleux, I.; et al. LKB1 regulates PRMT5 activity in breast cancer. *Int. J. Cancer* **2019**, *144*, 595–606.

84. Espejo, A.B.; Gao, G.; Black, K.; Gayatri, S.; Veland, N.; Kim, J.; Chen, T.; Sudol, M.; Walker, C.; Bedford, M.T. PRMT5 C-terminal phosphorylation modulates a 14-3-3/PDZ interaction switch. *J. Biol. Chem.* **2017**, *292*, 2255–2265.

85. Guderian, G.; Peter, C.; Wiesner, J.; Sickmann, A.; Schulze-Osthoff, K.; Fischer, U.; Grimmler, M. RioK1, a New Interactor of Protein Arginine Methyltransferase 5 (PRMT5), Competes with pICln for Binding and Modulates PRMT5 Complex Composition and Substrate Specificity. *J. Biol. Chem.* **2011**, *286*, 1976–1986.

86. Aggarwal, P.; Vaites, L.P.; Kim, J.K.; Mellert, H.; Gurung, B.; Nakagawa, H.; Herlyn,

M.; Hua, X.; Rustgi, A.K.; McMahon, S.B.; et al. Nuclear cyclin D1/CDK4 kinase regulates CUL4 expression and triggers neoplastic growth via activation of the PRMT5 methyltransferase. *Cancer Cell* **2010**, *18*, 329–340.

87. Zhang, H.T.; Zeng, L.F.; He, Q.Y.; Tao, W.A.; Zha, Z.G.; Hu, C.D. The E3 ubiquitin ligase CHIP mediates ubiquitination and proteasomal degradation of PRMT5. *Biochim. Biophys. Acta - Mol. Cell Res.* **2016**, *1863*, 335–346.

88. Li, Z.; Zhang, J.; Liu, X.; Li, S.; Wang, Q.; Chen, D.; Hu, Z.; Yu, T.; Ding, J.; Li, J.; et al. The LINC01138 drives malignancies via activating arginine methyltransferase 5 in hepatocellular carcinoma. *Nat. Commun.* **2018**, *9*, 1–14.

89. Lu, Y.-F.; Cai, X.-L.; Li, Z.-Z.; Lv, J.; Xiang, Y.; Chen, J.-J.; Chen, W.-J.; Sun, W.-Y.; Liu, X.-M.; Chen, J.-B. LncRNA SNHG16 Functions as an Oncogene by Sponging MiR-4518 and Up-Regulating PRMT5 Expression in Glioma. *Cell. Physiol. Biochem.* **2018**, *45*, 1975–1985.

90. Pal, S.; Vishwanath, S.N.; Erdjument-Bromage, H.; Tempst, P.; Sif, S. Human SWI/SNF-Associated PRMT5 Methylates Histone H3 Arginine 8 and Negatively Regulates Expression of ST7 and NM23 Tumor Suppressor Genes. *Mol. Cell. Biol.* **2004**, *24*, 9630–9645.

91. Scaglione, A.; Patzig, J.; Liang, J.; Frawley, R.; Bok, J.; Mela, A.; Yattah, C.; Zhang, J.; Teo, S.X.; Zhou, T.; et al. PRMT5-mediated regulation of developmental myelination. *Nat. Commun.* **2018**, *9*, 1–14.

92. Huang, S.; Litt, M.; Felsenfeld, G. Methylation of histone H4 by arginine methyltransferase PRMT1 is essential in vivo for many subsequent histone modifications. *Genes Dev.* **2005**, *19*, 1885–1893.

93. Migliori, V.; Müller, J.; Phalke, S.; Low, D.; Bezzi, M.; Mok, W.C.; Sahu, S.K.; Gunaratne, J.; Capasso, P.; Bassi, C.; et al. Symmetric dimethylation of H3R2 is a

newly identified histone mark that supports euchromatin maintenance. *Nat. Struct. Mol. Biol.* **2012**, *19*, 136–145.

94. Chiang, K.; Zielinska, A.E.; Shaaban, A.M.; Sanchez-Bailon, M.P.; Jarrold, J.; Clarke, T.L.; Zhang, J.; Francis, A.; Jones, L.J.; Smith, S.; et al. PRMT5 Is a Critical Regulator of Breast Cancer Stem Cell Function via Histone Methylation and FOXP1 Expression. *Cell Rep.* **2017**, *21*, 3498–3513.

95. Iberg, A.N.; Espejo, A.; Cheng, D.; Kim, D.; Michaud-Levesque, J.; Richard, S.; Bedford, M.T. Arginine methylation of the histone H3 tail impedes effector binding. *J. Biol. Chem.* **2008**, *283*, 3006–3010.

96. Kirmizis, A.; Santos-Rosa, H.; Penkett, C.J.; Singer, M.A.; Vermeulen, M.; Mann, M.; Bähler, J.; Green, R.D.; Kouzarides, T. Arginine methylation at histone H3R2 controls deposition of H3K4 trimethylation. *Nature* **2007**, *449*, 928–932.

97. Meister, G.; Eggert, C.; Bühler, D.; Brahms, H.; Kambach, C.; Fischer, U. Methylation of Sm proteins by a complex containing PRMT5 and the putative U snRNP assembly factor pICln. *Curr. Biol.* **2001**, *11*, 1990–1994.

98. Meister, G.; Fischer, U. Assisted RNP assembly: SMN and PRMT5 complexes cooperate in the formation of spliceosomal UsnRNPs. *EMBO J.* **2002**, *21*, 5853–5863.

99. Friesen, W.J.; Massenet, S.; Paushkin, S.; Wyce, A.; Dreyfuss, G. SMN, the product of the spinal muscular atrophy gene, binds preferentially to dimethylarginine-containing protein targets. *Mol. Cell* **2001**, *7*, 1111–1117.

100. Friesen, W.J.; Paushkin, S.; Wyce, A.; Massenet, S.; Pesiridis, G.S.; Van Duyne, G.; Rappsilber, J.; Mann, M.; Dreyfuss, G. The Methylosome, a 20S Complex Containing JBP1 and pICln, Produces Dimethylarginine-Modified Sm Proteins. *Mol. Cell. Biol.* **2001**, *21*, 8289–8300.

101. Bezzi, M.; Teo, S.X.; Muller, J.; Mok, W.C.; Sahu, S.K.; Vardy, L.A.; Bonday, Z.Q.;

Guccione, E. Regulation of constitutive and alternative splicing by PRMT5 reveals a role for Mdm4 pre-mRNA in sensing defects in the spliceosomal machinery. *Genes Dev.* **2013**, *27*, 1903–1916.

102. Allende-Vega, N.; Dayal, S.; Agarwala, U.; Sparks, A.; Bourdon, J.C.; Saville, M.K. P53 is activated in response to disruption of the pre-mRNA splicing machinery. *Oncogene* **2013**, *32*, 1–14.

103. Koh, C.M.; Bezzi, M.; Low, D.H.P.; Ang, W.X.; Teo, S.X.; Gay, F.P.H.; Al-Haddawi, M.; Tan, S.Y.; Osato, M.; Sabò, A.; et al. MYC regulates the core pre-mRNA splicing machinery as an essential step in lymphomagenesis. *Nature* **2015**, *523*, 96–100.

104. Dewaele, M.; Tabaglio, T.; Willekens, K.; Bezzi, M.; Teo, S.X.; Low, D.H.P.; Koh, C.M.; Rambow, F.; Fiers, M.; Rogiers, A.; et al. Antisense oligonucleotide-mediated MDM4 exon 6 skipping impairs tumor growth. *J. Clin. Invest.* **2016**, *126*, 68–84.

105. Gerhart, S. V.; Kellner, W.A.; Thompson, C.; Pappalardi, M.B.; Zhang, X.P.; Montes De Oca, R.; Penebre, E.; Duncan, K.; Boriack-Sjodin, A.; Le, B.; et al. Activation of the p53-MDM4 regulatory axis defines the anti-tumour response to PRMT5 inhibition through its role in regulating cellular splicing. *Sci. Rep.* **2018**, *8*.

106. Hamard, P.J.; Santiago, G.E.; Liu, F.; Karl, D.L.; Martinez, C.; Man, N.; Mookhtiar, A.K.; Duffort, S.; Greenblatt, S.; Verdun, R.E.; et al. PRMT5 Regulates DNA Repair by Controlling the Alternative Splicing of Histone-Modifying Enzymes. *Cell Rep.* **2018**, *24*, 2643–2657.

107. Inoue, M.; Okamoto, K.; Terashima, A.; Nitta, T.; Muro, R.; Negishi-Koga, T.; Kitamura, T.; Nakashima, T.; Takayanagi, H. Arginine methylation controls the strength of γc-family cytokine signaling in T cell maintenance. *Nat. Immunol.* **2018**, *19*, 1265–1276.

108. Rengasamy, M.; Zhang, F.; Vashisht, A.; Song, W.M.; Aguilo, F.; Sun, Y.; Li, S. De;

Zhang, W.; Zhang, B.; Wohlschlegel, J.A.; et al. The PRMT5/WDR77 complex regulates alternative splicing through ZNF326 in breast cancer. *Nucleic Acids Res.* **2017**, *45*, 11106–11120.

109. Gao, G.; Dhar, S.; Bedford, M.T. PRMT5 regulates IRES-dependent translation via methylation of hnRNP A1. *Nucleic Acids Res.* **2017**, *45*, 4359–4369.

110. Ren, J.; Wang, Y.; Liang, Y.; Zhang, Y.; Bao, S.; Xu, Z. Methylation of ribosomal protein S10 by protein-arginine methyltransferase 5 regulates ribosome biogenesis. *J. Biol. Chem.* **2010**, *285*, 12695–12705.

111. Xiao, W.; Chen, X.; Liu, L.; Shu, Y.; Zhang, M.; Zhong, Y. Role of protein arginine methyltransferase 5 in human cancers. *Biomed. Pharmacother.* **2019**, *114*, 108790.

112. Clarke, T.L.; Sanchez-Bailon, M.P.; Chiang, K.; Reynolds, J.J.; Herrero-Ruiz, J.; Bandeiras, T.M.; Matias, P.M.; Maslen, S.L.; Skehel, J.M.; Stewart, G.S.; et al. PRMT5-Dependent Methylation of the TIP60 Coactivator RUVBL1 Is a Key Regulator of Homologous Recombination. *Mol. Cell* **2017**, *65*, 900-916.e7.

113. Guo, Z.; Zheng, L.; Xu, H.; Dai, H.; Zhou, M.; Pascua, M.R.; Chen, Q.M.; Shen, B. Methylation of FEN1 suppresses nearby phosphorylation and facilitates PCNA binding. *Nat. Chem. Biol.* **2010**, *6*, 766–773.

114. He, W.; Ma, X.; Yang, X.; Zhao, Y.; Qiu, J.; Hang, H. A role for the arginine methylation of Rad9 in checkpoint control and cellular sensitivity to DNA damage.

115. Rehman, I.; Basu, S.M.; Das, S.K.; Bhattacharjee, S.; Ghosh, A.; Pommier, Y.; Das, B.B. PRMT5-mediated arginine methylation of TDP1 for the repair of topoisomerase I covalent complexes. *Nucleic Acids Res.* **2018**, *46*, 5601–5617.

116. Wei, H.; Wang, B.; Miyagi, M.; She, Y.; Gopalan, B.; Huang, D. Bin; Ghosh, G.; Stark, G.R.; Lu, T. PRMT5 dimethylates R30 of the p65 subunit to activate NF-?B. *Proc. Natl. Acad. Sci. U. S. A.* **2013**, *110*, 13516–13521.

117. Tabata, T.; Kokura, K.; ren Dijke, P.; Ishii, S. Ski co-repressor complexes maintain the basal repressed state of the TGF-β target gene, SMAD7, via HDAC3 and PRMT5. *Genes to Cells* **2009**, *14*, 17–28.

118. Fu, T.; Lv, X.; Kong, Q.; Yuan, C. A novel SHARPIN-PRMT5-H3R2me1 axis is essential for lung cancer cell invasion. *Oncotarget* **2017**, *8*, 54809–54820.

119. Hsu, J.M.; Chen, C. Te; Chou, C.K.; Kuo, H.P.; Li, L.Y.; Lin, C.Y.; Lee, H.J.; Wang, Y.N.; Liu, M.; Liao, H.W.; et al. Crosstalk between Arg 1175 methylation and Tyr 1173 phosphorylation negatively modulates EGFR-mediated ERK activation. *Nat. Cell Biol.* **2011**, *13*, 174–181.

120. Calabretta, S.; Vogel, G.; Yu, Z.; Choquet, K.; Darbelli, L.; Nicholson, T.B.; Kleinman, C.L.; Richard, S. Loss of PRMT5 Promotes PDGFRα Degradation during Oligodendrocyte Differentiation and Myelination. *Dev. Cell* **2018**, *46*, 426-440.e5.

121. Alinari, L.; Mahasenan, K.V.; Yan, F.; Karkhanis, V.; Chung, J.; Smith, E.M.; Quinion, C.; Smith, P.L.; Kim, L.; Patton, J.T.; et al. Selective inhibition of protein arginine methyltransferase 5 blocks initiation and maintenance of B-cell transformation. *Blood* **2015**, *125*, 2530–2543.

122. Panfil, A.R.; Al-Saleem, J.; Howard, C.M.; Mates, J.M.; Kwiek, J.J.; Baiocchi, R.A.; Green, P.L. PRMT5 is upregulated in HTLV-1-mediated T-Cell transformation and selective inhibition alters viral gene expression and infected cell survival. *Viruses* **2015**, *8*, 1–20.

123. Zhang, W.; Chen, J.; Wu, M.; Zhang, X.; Zhang, M.; Yue, L.; Li, Y.; Liu, J.; Li, B.; Shen, F.; et al. PRMT5 restricts hepatitis B virus replication through epigenetic repression of covalently closed circular DNA transcription and interference with pregenomic RNA encapsidation. *Hepatology* **2017**, *66*, 398–415.

124. Lubyova, B.; Hodek, J.; Zabransky, A.; Prouzova, H.; Hubalek, M.; Hirsch, I.; Weber,

J. PRMT5: A novel regulator of Hepatitis B virus replication and an arginine methylase of HBV core. *PLoS One* **2017**, *12*, 1–28.

125. Strahan, R.C.; McDowell-Sargent, M.; Uppal, T.; Purushothaman, P.; Verma, S.C. *KSHV encoded ORF59 modulates histone arginine methylation of the viral genome to promote viral reactivation*; 2017; Vol. 13; ISBN 1111111111.

126. Murakami, H.; Suzuki, T.; Tsuchiya, K.; Gatanaga, H.; Taura, M.; Kudo, E.; Okada, S.; Takei, M.; Kuroda, K.; Yamamoto, T.; et al. Protein Arginine N-methyltransferases 5 and 7 Promote HIV-1 Production. *Viruses* **2020**, *12*, 355.

127. Sato, H.; Watanuki, S.; Bai, L.; Borjigin, L.; Ishizaki, H.; Matsumoto, Y.; Hachiya, Y.; Sentsui, H.; Aida, Y. A sensitive luminescence syncytium induction assay (LuSIA) based on a reporter plasmid containing a mutation in the glucocorticoid response element in the long terminal repeat U3 region of bovine leukemia virus. *Virol. J.* **2019**, *16*, 66.

128. Miyasaka, T.; Takeshima, S.N.; Jimba, M.; Matsumoto, Y.; Kobayashi, N.; Matsuhashi, T.; Sentsui, H.; Aida, Y. Identification of bovine leukocyte antigen class II haplotypes associated with variations in bovine leukemia virus proviral load in Japanese Black cattle. *Tissue Antigens* **2013**, *81*, 72–82.

129. Bedford, M.T.; Clarke, S.G. Protein arginine methylation in mammals: who, what, and why. *Mol. Cell* **2009**, *33*, 1–13.

130. Fabbrizio, E.; El Messaoudi, S.; Polanowska, J.; Paul, C.; Cook, J.R.; Lee, J.-H.; Negre, V.; Rousset, M.; Pestka, S.; Le Cam, A.; et al. Negative regulation of transcription by the type II arginine methyltransferase PRMT5. *EMBO Rep.* **2002**, *3*, 641–5.

131. Bieberich, E. Synthesis, Processing, and Function of N-glycans in N-glycoproteins. In *Advances in neurobiology*; NIH Public Access, 2014; Vol. 9, pp. 47–70.

132. N-Glycans - Essentials of Glycobiology - NCBI Bookshelf Available online: https://www.ncbi.nlm.nih.gov/books/NBK20720/ (accessed on Apr 18, 2020).

133. Freeze, H.H.; Kranz, C. Endoglycosidase and glycoamidase release of N-linked glycans. *Curr. Protoc. Mol. Biol.* **2010**, *2010*.

134. Pique, C.; Pham, D.; Tursz, T.; Dokhélar, M.C. Human T-cell leukemia virus type I envelope protein maturation process: requirements for syncytium formation. *J. Virol.* **1992**, *66*, 906–13.

135. Gruters, R.A.; Neefjes, J.J.; Tersmette, M.; De Goede, R.E.Y.; Tulp, A.; Huisman, H.G.; Miedema, F.; Ploegh, H.L. Interference with HIV-induced syncytium formation and viral infectivity by inhibitors of trimming glucosidase. *Nature* **1987**, *330*, 74–77.

136. Pal, S.; Baiocchi, R.A.; Byrd, J.C.; Grever, M.R.; Jacob, S.T.; Sif, S. Low levels of miR-92b/96 induce PRMT5 translation and H3R8/H4R3 methylation in mantle cell lymphoma. *EMBO J.* **2007**, *26*, 3558–3569.

137. Wang, L.; Pal, S.; Sif, S. Protein Arginine Methyltransferase 5 Suppresses the Transcription of the RB Family of Tumor Suppressors in Leukemia and Lymphoma Cells. *Mol. Cell. Biol.* **2008**, *28*, 6262–6277.

138. Chung, J.; Karkhanis, V.; Tae, S.; Yan, F.; Smith, P.; Ayers, L.W.; Agostinelli, C.; Pileri, S.; Denis, G. V.; Baiocchi, R.A.; et al. Protein arginine methyltransferase 5 (PRMT5) inhibition induces lymphoma cell death through reactivation of the retinoblastoma tumor suppressor pathway and polycomb repressor complex 2 (PRC2) Silencing. *J. Biol. Chem.* **2013**, *288*, 35534–35547.

139. Nicholas, C.; Yang, J.; Peters, S.B.; Bill, M.A.; Baiocchi, R.A.; Yan, F.; Sïf, S.; Tae, S.; Gaudio, E.; Wu, X.; et al. PRMT5 is upregulated in malignant and metastatic melanoma and regulates expression of MITF and p27(Kip1.). *PLoS One* **2013**, *8*, e74710.

140. Deery, M.J.; Vieira, G.C.; Heesom, K.J.; Zheng, Y.G.; Von Wallwitz-Freitas, L.; Brown, K.W.; Catchpoole, D.; Malik, K.; Malik, S.; Melegh, Z.; et al. Protein arginine methyltransferase 5 is a key regulator of the MYCN oncoprotein in neuroblastoma cells. *Mol. Oncol.* **2014**, *9*, 617–627.

141. Bao, X.; Zhao, S.; Lius, T.; Liu, Y.; Liu, Y.; Yang, X. Overexpression of PRMT5 Promotes Tumor Cell Growth and Is Associated with Poor Disease Prognosis in Epithelial Ovarian Cancer. *J. Histochem. Cytochem.* **2013**, *61*, 206–217.

142. Hu, D.; Gur, M.; Zhou, Z.; Gamper, A.; Hung, M.C.; Fujita, N.; Lan, L.; Bahar, I.; Wan, Y. Interplay between arginine methylation and ubiquitylation regulates KLF4-mediated genome stability and carcinogenesis. *Nat. Commun.* **2015**, *6*, 1–15.

143. Kanda, M.; Shimizu, D.; Fujii, T.; Tanaka, H.; Shibata, M.; Iwata, N.; Hayashi, M.; Kobayashi, D.; Tanaka, C.; Yamada, S.; et al. Protein arginine methyltransferase 5 is associated with malignant phenotype and peritoneal metastasis in gastric cancer. *Int. J. Oncol.* **2016**, *49*, 1195–1202.

144. Fabbrizio, E.; Messaoudi, S. El; Polanowska, J.; Paul, C.; Cook, J.R.; Lee, J.; Nègre, V.; Rousset, M.; Pestka, S.; Cam, A. Le; et al. Negative regulation of transcription by the type II arginine methyltransferase PRMT5. *EMBO Rep.* **2002**, *3*, 641–645.

145. Pierard, V.; Guiguen, A.; Colin, L.; Wijmeersch, G.; Vanhulle, C.; Van Driessche, B.; Dekoninck, A.; Blazkova, J.; Cardona, C.; Merimi, M.; et al. DNA cytosine methylation in the bovine leukemia virus promoter is associated with latency in a lymphoma-derived B-cell line: Potential involvement of direct inhibition of camp-responsive element (CRE)-binding protein/cre modulator/activation transcription factor binding. *J. Biol. Chem.* **2010**, *285*, 19434–19449.

146. Merezak, C.; Reichert, M.; Van Lint, C.; Kerkhofs, P.; Portetelle, D.; Willems, L.; Kettmann, R. Inhibition of Histone Deacetylases Induces Bovine Leukemia Virus

Expression In Vitro and In Vivo. *J. Virol.* **2002**, *76*, 5034–5042.

147. Achachi, A.; Florins, A.; Gillet, N.; Debacq, C.; Urbain, P.; Foutsop, G.M.; Vandermeers, F.; Jasik, A.; Reichert, M.; Kerkhofs, P.; et al. Valproate activates bovine leukemia virus gene expression, triggers apoptosis, and induces leukemia/lymphoma regression in vivo. *Proc. Natl. Acad. Sci. U. S. A.* **2005**, *102*, 10309–10314.

148. van Kooyk, Y.; Kalay, H.; Garcia-Vallejo, J.J. Analytical tools for the study of cellular glycosylation in the immune system. *Front. Immunol.* **2013**, *4*, 1–6.

149. Go, E.P.; Liao, H.X.; Alam, S.M.; Hua, D.; Haynes, B.F.; Desaire, H. Characterization of host-cell line specific glycosylation profiles of early transmitted/founder HIV-1 gp120 envelope proteins. *J. Proteome Res.* **2013**, *12*, 1223–1234.

150. Montefiori, D.C.; Robinson, W.E.; Mitchell, W.M. Role of protein N-glycosylation in pathogenesis of human immunodeficieny virus type 1. *Proc. Natl. Acad. Sci. U. S. A.* **1988**, *85*, 9248–9252.

151. Zhang, M.; Gaschen, B.; Blay, W.; Foley, B.; Haigwood, N.; Kuiken, C.; Korber, B. Tracking global patterns of N-linked glycosylation site variation in highly variable viral glycoproteins: HIV, SIV, and HCV envelopes and influenza hemagglutinin. *Glycobiology* **2004**, *14*, 1229–1246.

152. Rizzo, G.; Forti, K.; Serroni, A.; Cagiola, M.; Baglivo, S.; Scoccia, E.; De Giuseppe, A. Single N-glycosylation site of bovine leukemia virus SU is involved in conformation and viral escape. *Vet. Microbiol.* **2016**, *197*, 21–26.

153. Leonard, S.; Gordon, N.; Smith, N.; Rowe, M.; Murray, P.G.; Woodman, C.B. Arginine methyltransferases are regulated by Epstein-Barr virus in B cells and are differentially expressed in Hodgkin's lymphoma. *Pathogens* **2012**, *1*, 52–64.